HHS Public Access

Author manuscript

J Comp Neurol. Author manuscript; available in PMC 2017 December 15.

Published in final edited form as:

J Comp Neurol. 2016 December 15; 524(18): 3696–3716. doi:10.1002/cne.24025.

Retinal pigment epithelial integrity is compromised in the developing albino mouse retina

Lena Iwai[1], **Anna Ramos**[1], **Ari Schaler**[1], **Samuel Weinreb**[1], **Richard Blazeski**[1], and **Carol Mason**[1,2,3]

[1]Department of Pathology and Cell Biology, Columbia University, New York, NY, 10032, USA

[2]Department of Neuroscience, Columbia University, New York, NY, 10032, USA

[3] Department of Ophthalmology, College of Physicians and Surgeons, Columbia University, New York, NY, 10032, USA

Abstract

In the developing murine eye, melanin synthesis in the retinal pigment epithelium (RPE) coincides with neurogenesis of retinal ganglion cells (RGCs). Disruption of pigmentation in the albino RPE is associated with delayed neurogenesis in the ventrotemporal retina, the source of ipsilateral RGCs, and a reduced ipsilateral RGC projection.

To begin to unravel how melanogenesis and the RPE regulate RGC neurogenesis and cell subpopulation specification, we have compared the features of albino and pigmented mouse RPE cells during the period of RGC neurogenesis (embryonic day,E, 12.5 to 18.5) when the RPE is closely apposed to developing RGC precursors. At E12.5 and E15.5, although albino and pigmented RPE cells express RPE markers Otx2 and Mitf similarly, albino RPE cells are irregularly shaped and have fewer melanosomes compared with pigmented RPE cells. The adherens junction protein P-cadherin appears loosely distributed within the albino RPE cells rather than tightly localized on the cell membrane as in pigmented RPE. Connexin 43 (gap junction protein) is expressed in pigmented and albino RPE cells at E13.5 but at E15.5 albino RPE cells have fewer small connexin 43 puncta, and a larger fraction of phosphorylated connexin 43 at serine 368. These results suggest that the lack of pigment in the RPE results in impaired RPE cell integrity and communication via gap junctions between RPE and neural retina during RGC neurogenesis. Our findings should pave the way for further investigation of the role of RPE in regulating RGC development toward achieving a proper RGC axon decussation.

Graphical abstract

Corresponding author: Carol Mason, Department of Pathology and Cell Biology, College of Physicians and Surgeons, Columbia University, 14-509 P&S Bldg., 630 W. 168th St., New York, NY 10032, 1-212-305-2105, cam4@cumc.columbia.edu.

Conflict of interest

The authors have no conflict of interest.

Role of authors

All authors had full access to all the data in the study and take responsibility for the integrity of the data and the accuracy of the data analysis. Study concept and design: LI and CM. Data acquisition and analysis of data: LI, AR, AS, SW and RB. Interpretation of data: LI and CM. Drafting of the manuscript: LI and CM. Obtained funding: LI and CM.

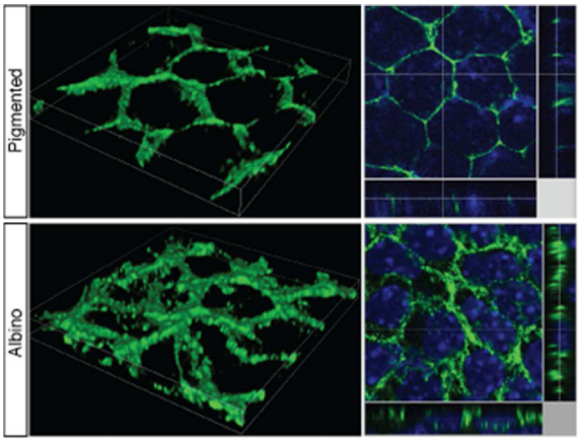

Keywords

melanosomes; gap junctions; connexin 43; P-cadherin; Zic2; retinal ganglion cells; RRID: AB_638639; RRID: AB_476857; RRID: AB_86574; RRID: AB_2315623

Introduction

The retinal pigment epithelium (RPE) is a monolayer of polarized and highly specialized pigmented cells that are situated scleral to the neural retina. In the postnatal vertebrate eye, an intact and functional RPE is crucial for photoreceptor outer segment phagocytosis, photoreceptor survival, and retinoid metabolism. The cell biology of the RPE has been studied most extensively in the adult retina in the normal and diseased state, as in age-related macular degeneration (Sparrow et al., 2010; Bertolotti et al., 2014), but less is known about the RPE during embryonic retinal development.

During early eye development, after invagination of the eye anlage, the optic vesicle differentiates into two closely apposed layers, the RPE and the neural retina, regulated by a consortium of growth factors and transcription factors (Raymond and Jackson, 1995; Martinez-Morales et al., 2004; Bharti et al., 2006; Fuhrmann et al., 2014). Genetic ablation of the RPE during embryogenesis results in disrupted morphogenesis and lamination of the neural retina (Raymond and Jackson, 1995), suggesting that the RPE is required for proper neural retinal development. However, how the RPE and developing neural retinal layers interact to influence further retinal development is poorly understood. One intriguing feature of the developing RPE is that intercellular junctions are positioned between RPE cells and between RPE and neural retinal precursors including RGC precursors. These junctions could be important conduits for signaling molecules that regulate both RPE integrity and the development of the neural retina (Jeffery, 1998; Cook and Becker, 2009).

Albinism is a disorder characterized by disrupted melanosomes (the pigment-containing organelle in the RPE) and/or melanin synthesis. A hallmark of all forms of albinism (*tyrosinase* mutations in oculocutaneous albinism 1, OCA1; disruption of melanosome maturation in ocular albinism type 1, OA1; and in other pigment and lysosomal genetic disorders) is a reduction in the proportion of ipsi- and contralateral RGC axonal projections,

leading to impaired binocular vision. The cellular and molecular link between defects in the RPE and the imbalance of ipsi- and contralateral RGC projections has long been a puzzle.

As the RPE acquires pigment beginning at embryonic day (E) 11.5, RGCs are born and differentiate into two subpopulations, one projecting their axons to targets on the ipsilateral side of the brain and the other projecting contralaterally. In mice, the ipsilateral projecting RGCs develop in the ventrotemporal (VT) retina between E14.5 and E16.5 (Dräger, 1985a; Petros et al., 2008; Erskine and Herrera, 2014). Transcription factors and axon guidance receptors regulate the cell fate and projection of the ipsi- and contralateral RGCs (Herrera et al., 2003; Williams et al., 2003; Pak et al., 2004; Williams et al., 2006; Badea and Nathans, 2011; Erskine et al., 2011; Kuwajima et al., 2012). In the albino mouse retina, specifically in the VT sector, fewer ipsilateral RGCs (Zic2-positive) are born between E13.5 and E14.5, and more contralateral RGCs (Islet 2-positive) at E17.5 (Bhansali et al., 2014). Further, the peak of RGC genesis in the albino VT retina is delayed by approximately a day compared with pigmented retina (Bhansali et al., 2014). Anterograde tracing of RGC axons projecting to the dorsal lateral geniculate nucleus (dLGN) in the postnatal albino mouse has revealed an aberrant patch of contralateral fibers from the VT retina, segregated but adjacent to the terminus of contralateral RGCs that normally extend from VT retina late in development (Rebsam et al., 2012). This aberrant cluster of axon terminals may reflect an increase RGCs in VT retina specified to a contralateral fate. These results suggest that disruption of pigmentation in the RPE is associated with altered RGC production, subpopulation specificity (e.g., ipsi- vs contralateral RGCs), and consequently, the reduced ipsilateral projection to targets that characterizes albinism.

Previous studies have investigated the cellular features of the developing rat (Kuwabara and Weidman, 1974) and mouse (Bodenstein and Sidman, 1987) RPE, but without detailed comparison of pigmented and albino RPE. In the albino embryonic rat, melanosomes lacking pigment are located in the apical aspect of RPE cells until a few weeks postnatally, and ultimately disappear (Kuwabara and Weidman, 1974). Maturation and size defects have been found in embryonic and postnatal mouse RPE, mainly in the *Oa1* mutant (Cortese et al., 2005; Palmisano et al., 2008; Young et al., 2008; Giordano et al., 2009). Aberrant cell shape and gap junction protein connexin43 (Cx43) expression was reported in the postnatal albino rat RPE (Tibber et al., 2007; Adams et al., 2010). In other cell types such as cardiac myocytes, the phosphorylation state of gap junctions is linked to proliferation status and also affects gap junction gating (Solan and Lampe, 2009; 2014). These cellular features have not been examined in the embryonic mouse RPE with regard to timing of RGC neurogenesis or the location of progenitors giving rise to ipsilaterally- or contralaterally- projecting RGCs.

Here we use albinism as a genetic model to understand the cellular interactions between the RPE and neural retina and hypothesize that these interactions are critical for proper specification of ipsi-and contralateral RGCs during neurogenesis. We analyzed RPE in pigmented and albino mouse retina E12.5 to E18.5, and demonstrate that RPE cell morphology, melanosome number and distribution, adherens junction protein (P-cadherin) distribution, and gap junction protein (Cx43) expression and phosphorylation are disrupted in the embryonic albino mouse RPE. These perturbations could affect RPE integrity, and

potentially, RPE-neural retinal communication that could produce disrupted neurogenesis and axon-target specificity seen in the albino.

Materials and Methods

Animals

B6 (Cg)- *Tyr* $^{C\text{-}2J}$/J mice were obtained from The Jackson Laboratory (RRID:IMSR_JAX:000058) and maintained in a timed-pregnancy breeding colony at Columbia University. Conditions and procedures were approved by the Columbia University Institutional Animal Care and Use Committee, in protocols AC-AAAG9259, AC-AAAG8702. Heterozygous mice ($Tyr^{+/c2j}$) were crossed with homozygous tyrosinase mutants ($Tyr^{c2j/c2j}$) to generate litters containing homozygous $Tyr^{c2j/c2j}$ embryos ("albino") and heterozygous $Tyr^{+/c2j}$ embryos ("pigmented"). Pigmented littermates were used as controls for albino embryos. Females were checked for vaginal plugs at approximately noon each day. Embryonic day (E) 0.5 corresponds to the day when the vaginal plug was detected. To collect embryos, pregnant dams were injected with ketamine and xylazine (80m/kg and 10 mg/kg, respectively) intraperitoneally.

Immunohistochemistry (IHC)

The primary antibodies used on both sections and whole mounts are described in Table 1. Secondary antibodies used included donkey anti-rabbit Alexa488, donkey anti-rabbit Alexa594, donkey anti-goat Alexa488 and donkey anti-mouse IgG Alexa488 (Life Technologies), and donkey anti-goat IgG Cy3 and donkey anti-rat Cy3 (Jackson ImmunoResearch). All secondary antibodies were used at a 1:500 dilution. Antigen retrieval was performed for anti-Mitf (Thermo Scientific, Cat# MS-771-P0, RRID:AB_141540) staining by incubating slides in 10mM Sodium citrate, 0.05% Tween-20, pH6.0 at 95–100°C for 20 min prior to the blocking step for IHC.

For IHC of retinal sections, heads from E12.5, E13.5, E15.5, or E17.5 embryos were fixed by immersion in 4% paraformaldehyde (PFA) 1 hour for Mitf and P-cadherin (Invitrogen, Cat# 132000Z, RRID:AB_86574) staining or overnight for Cx43 (Santa Cruz Biotechnology, Cat# sc-6560, RRID:AB_638639) staining, then cryoprotected in 10% sucrose for tissue fixed 1 hour or 30% sucrose for tissue fixed overnight in phosphate buffered saline (PBS) for 24–48 hours at 4°C. The heads were cut into 14 μm thick coronal sections using a Leica cryostat.

To reduce the concentration of melanin in pigmented RPE, which masks the immunohistochemical signal, sections fixed overnight from both genotypes were bleached following protocols from Foss et al. (1995) and Orchard and Calonje (1998). In brief, sections were incubated with 0.25% $KMnO_4$ (Sigma 23851) in PBS for 30 minutes (min), washed in PBS, and then incubated in 1% oxalic acid (Sigma O-0376) for 1 min and washed again in PBS. The bleached sections were then blocked for IHC in 1% Bovine Serum Albumin (BSA), 0.2% Triton X-100 in PBS, and incubated overnight at 4°C with primary antibodies in 0.1% BSA, 0.2% Triton X-100 in PBS. Sections were washed in PBS and then incubated for 2 hours with secondary antibodies in 0.1% BSA, 0.2% Triton X-100 in PBS at

room temperature. Cell nuclei were counterstained with Hoechst 33258 (Life Technologies H3569), 1 μg/ml in PBS.

For IHC on RPE whole mounts, embryos were collected at E15.5 and E17.5. Heads were fixed by immersion in 4% PFA in PBS for 1 hour at 4°C and rinsed 3 times in PBS at 4°C. A small radial slit was made at the dorsal pole of the retina for future orientation. The cornea was cut, the lens was removed, and the RPE with extraocular tissue attached was dissected free from the head. The neural retina was detached from the RPE and extraocular tissue was removed. The dissected RPE eyecups were processed for IHC as described above but without bleaching.

For 3D reconstruction of IHC images of RPE whole mounts, a merged stack with 0.15 μm steps was acquired using a Nikon A1 scanning confocal microscope.

Electron Microscopy

Electron microscopy of RPE from intact embryos was performed as follows: For E13.5 embryos, pregnant mice were anesthetized as described above and the dam perfused transcardially with cold 3% glutaraldehyde in 0.1 M phosphate buffer (PB); embryos were collected and fixed by immersion overnight in cold 3% glutaraldehyde in 0.1M PB. E16.5 and 18.5 embryos were dissected from dams anaesthetized as described above and perfused transcardially with the same fixative. Embryo heads were then incubated overnight in fixative at 4° C. The heads were embedded in 3% agarose and coronal sections cut at 100 μm with a Leica vibratome. Using a microwave for electron microscopy (Pelco model 3451 system with coldspot), the 100 μm vibratome sections were post-fixed with 1% osmium tetroxide in 0.1M PB for 2 × 40 seconds (sec) in fresh osmium and washed 3 × 10 min in 0.1M PB. Sections were next dehydrated for 40 sec each in an ethanol series of 50%, 70%, 95%, and 2 × 100% in the microwave. Sections were infiltrated in the microwave for 15 min with a 1:1 mixture of 100% epon (Embed 812, Electron Microscopy Sciences) and 100% ethanol, and then infiltrated for 2 × 15 min in 100% epon. Sections were mounted between plastic slides with 100% epon and polymerized overnight at 60°C. The polymerized epon wafers were then separated from the plastic slides and placed flat on a glass slide to photograph the sections. One 100 μm thick section at the level of the optic nerve was selected from each embryo, cut from the epon wafer and remounted on a blank Beem capsule block and polymerized overnight at 60° C. The remounted sections were then trimmed and sectioned at 10 μm with a diamond HistoKnife (Diatome) using an ultramicrotome. Serial 10 μm thick sections were collected and mounted in immersion oil on a glass slide, coverslipped, and photographed. One of the 10 μm sections at the middle of the series was selected for each embryo and washed 3 × 15 sec in 95% ethanol to remove excess oil. The section was then blotted with lens paper, remounted on a drop of epon on a flat smooth-surfaced blank block, and polymerized overnight at 60°C, with a spring tension apparatus to keep section flat against a plastic slide. The areas of interest (dorsal and ventral RPE) in the section were then trimmed and cut into 60 nm sections using an ultramicrotome with a Diatome diamond knife. The ultrathin sections were collected onto a Formvar coated slot grid, stained with uranyl acetate and lead citrate, and examined with a JEOL 1200EX electron microscope.

Quantification of melanosomes

The melanosome number and distribution in the apical versus basal zone of RPE cells in pigmented and albino retina was analyzed in electron micrographs. In the first 10 μm section posterior to the optic nerve, dorsal and ventral RPE was analyzed over a distance of 480 μm from the central border of the ciliary margin zone (CMZ) toward the central retina at E13.5 and E16.5, and within 640 μm for E18.5. The peripheral edge of the RPE was circumscribed by the peripheral-most border of the RGC layer, as labeled with antibodies to Islet 1/2 (dorsal) or Zic2 (ventral) in reference retinal sections. The basal aspect of the RPE was defined by the presence of basal lamina, and the apical aspect was defined by the interface with the neural retina. The border between the apical and basal regions was drawn at a half-distance between the apical and basal surfaces as described previously (Cortese et al., 2005). In the albino RPE, melanosomes were distinguished from holes in the tissue by intraluminal membranes in the melanosome ghosts. At each age, 3 pigmented embryos and 3 albino littermate embryos were analyzed (2 pairs of embryos from litter A and 1 pair of embryos from litter B). One eye from each embryo was analyzed.

Quantification of RPE cell morphology

Stained RPE whole mounts (one eye from each embryo) were imaged using a Zeiss AxioImager M2 microscope equipped with ApoTome, AxioCam camera, and Neurolucida software V11 (MicroBrightField Systems, RRID: SCR_001775). A merged stack with 2μm steps was acquired using the ApoTome and a 20× objective. Using ImageJ (https://imagej.nih.gov/ij/, RRID: nif-0000–30467), two adjacent regions (100 × 100 μm) from the same quadrant (dorsal or ventral RPE) were selected (250–300 μm from the border of the CMZ, Fig. 2A). This is because if a unitary area (the sum of these two regions) was selected, detecting the field by CellProfiler Image Analysis Software (http://www.cellprofiler.org, RRID: nif-0000–00280) was less accurate. To quantify cell shape parameters, images of cells outlined by ZO-1 (zona occludens 1, a tight junction protein) were first modified by subtracting background noise in ImageJ by setting the rolling ball radius to 50.0 pixels and uploading the data into CellProfiler. CellProfiler modified the ZO-1 images as follows: the illumination function, used to correct images for uneven illumination and background, was calculated for each ZO-1 image: the image was then smoothened using the fit polynomial method, rescaled, and its intensity inverted. Objects (i.e., RPE cells outlined by ZO-1-positive cell membranes) were identified by CellProfiler and edited manually for accuracy. The cell shape parameters defined by CellProfiler (area, eccentricity, and solidity) were quantified: the area equals the actual number of pixels in the individual ZO-1 outlined RPE cells; solidity is the proportion of the object area filling a convex envelope of best fit around the object; eccentricity is the measure of elongation of an ellipse fitted to each cell, i.e, the fractional distance of each focus of that ellipse from the midpoint of its major axis. In addition, compactness, extent, perimeter and form factor were measured and compared in albino and pigmented RPE. Compactness is the variance of the radial distance of the object's pixels from the centroid divided by the area. Perimeter is the total number of pixels around the boundary of each region in the image. Form factor is calculated as $4 \times \pi \times \text{area}/\text{perimeter}^2$. Form factor equals 1 for a perfectly circular object. Details of the calculation methods used by CellProfiler are available at http://www.cellprofiler.org.

Quantification of Cx43 expression and distribution

For Cx43 expression level and distribution analysis, one 14 μm cryostat section cut frontally through the optic nerve and a second section taken after the third section posterior to the optic nerve, were labeled with Cx43 and Na^+/K^+ ATPase and then photographed on a Nikon A1 scanning confocal microscope. To determine the region of the RPE adjacent to the developing ipsilateral and contralateral RGCs, the sections immediately preceding those stained with Cx43 and Na^+/K^+ ATPase were labeled with antibodies to Zic2 and Islet1/2 and photographed to serve as a reference section.

All measurements pertaining to Cx43 were performed using FIJI (http://fiji.sc/, RRID: SciRes 000137). Using Na^+/K^+ ATPase labeling to visualize the outlines of RPE cells, a region of interest (ROI) was selected in the RPE. In the ventrotemporal (VT) region, the ROI began at the RPE cell adjacent to the most peripheral cell double labeled with antibodies to Zic2 (ipsilateral RGCs) and Islet1/2 (differentiated RGCs) in the neural retina (as viewed in the reference section) and extended 200 μm centrally. In the dorsotemporal (DT) region, the ROI began at the cell adjacent to the first Islet1/2-positive cell in the neural retina (as viewed in the reference section) and extended 200 μm centrally. The background fluorescent signal was calculated for each section and subtracted before analysis by setting a threshold equal in value to the background signal. The background value was measured by adding the mean gray value (average pixel intensity) within a 100 μm × 100 μm box in the central ventral neural retina, which lacks Cx43 expression, to four times the standard deviation of this value. After setting the threshold, the integrated density (sum of pixel intensities) of the Cx43 labeling was measured within the RPE ROI. Cx43 expression level was calculated by dividing the integrated density within the RPE ROI by the area of this region in order to account for differences in area of the ROIs between sections.

To quantify the distribution of Cx43 expression, the RPE ROI was divided into apical and non-apical sectors. Because we aimed to study the relationship between the apical surface of the RPE cell and the neural retina, we decided to focus on the apical region, defined as the most apical third of the RPE cells (at the neural retinal side) and the non-apical side as the remaining two-thirds (at the basal lamina aspect), as previously described (Palmisano et al., 2008). Cx43 expression levels were calculated for both the apical and non-apical regions. To calculate the percentage of expression located apically and non-apically, each Cx43 expression level value was divided by the sum of expression in both sectors.

The Analyze Particles command in FIJI was used to quantify Cx43 particle number and size. The threshold of pixel intensity was set as described above. The acceptable diameter range of particles was set as 0 to infinity; circularity was set as 0.00 to 1.00. $n = 5$ pigmented embryos and 5 albino littermate embryos from 3 different litters at E13.5; 7 pigmented embryos and 7 albino littermate embryos from 5 different litters at E15.5. One eye from each embryo was analyzed.

Western blot analysis

RPE was collected from albino and pigmented embryos at E13.5 and E15.5 as described above for preparation of RPE whole mounts, but the tissue was not fixed. Both eyes of 4–5

pigmented embryos from 2–3 litters were pooled as one RPE sample at each age. The same number of eyes was collected from albino embryo littermates. RPE were lysed and the collected protein samples were separated and transferred to nitrocellulose membranes as described previously (Perron and Dodd, 2009). The nitrocellulose membranes were subsequently blocked in 5% BSA/0.1% Tween-20 for 1 hour at room temperature and incubated overnight at 4°C with mouse anti-vinculin (Sigma-Aldrich, Cat# V9131, RRID: AB_477629) and either rabbit anti-Cx43 (RRID: AB_476857) or rabbit anti-Phospho-Cx43 (Cell Signaling Technology, Cat# 3511S, RRID: AB_2110169) in 5% BSA/0.1% Tween-20. After 4 washes in PBS/0.1% Tween-20, the membranes were incubated for 50 minutes with fluorescently labeled secondary goat anti-mouse and goat anti-rabbit antibodies (1:15000, LI-COR Biosciences, gift of Dr. Ismael Perez, Columbia University) in 5% BSA/0.1% Tween-20. Membranes were washed 3 times in PBS/0.1% Tween-20 and once in PBS alone to remove residual Tween-20. Membranes were imaged using the Odyssey Infrared Imaging System (LI-COR Biosciences). Experiments were repeated at least 3 times in different RPE samples and gave consistent results. To quantify protein bands, densimetric analysis by ImageJ Gel analysis function was performed.

Antibody characterization

Primary antibodies used in IHC and western blot (WB) are described in Table 1. The anti-Zic2 antibody (RRID: AB_2315623; JCN antibody database #7501) was produced in rabbit against the C-terminal segment, which is not present in the closely related Zic1 and Zic3 proteins (Brown et al., 2003). Chinese hamster ovary (CHO) cells were made to express Zic1, Zic2, or Zic3 by transfection with cDNA plasmids, and the Zic2-specific antiserum interacted strongly with the $Zic2^+$ cells, but only weakly or not at all with the $Zic1^+$ and $Zic3^+$ cells as demonstrated by immunofluorescent staining, which was localized to the nuclei. Equivalent transfection efficiency in all three dishes was confirmed by co-transfection with a lac-Z plasmid, as well as by immunofluorescent staining with a pan-Zic2 antibody. Zic2 specificity was further verified by Western blot analysis of lysates from the transfected CHO cells, in which a band (55 kDa) appeared only for the $Zic2^+$ cells and immunohistochemistry using mouse embryo tissue (Brown et al., 2003).

Monoclonal antibody 39.4D5 (RRID: AB_528173; JCN antibody database #20–24) recognizes a 25kDa truncated rat Islet-1 protein (c-terminal Islet-1) on Western blot (Thor et al., 1991) corresponding to carboxy-terminal residues 178–349 (Karlsson et al., 1990). This antibody also recognizes Islet 2 (Developmental Hybridoma Bank); (Tsuchida et al., 1994). The specificity of antibody was determined by comparison of the labeling patterns obtained by immunocytochemistry and by *in situ* hybridization (Tsuchida et al., 1994).

The goat anti-connexin 43 (Cx43) antibody (Santa Cruz Biotechnology, Cat# sc-6560, RRID: AB_638639) recognized single bands of 43 kDa in Western blot analyses of both untreated and lambda protein phosphatase-treated rat heart tissue extracts. Immunoperoxidase staining of human heart muscle tissue showed cytoplasmic and intercalataed disc staining of myocytes (Santa Cruz Biotechnology). The antibody is specific to non-phosphorylated Cx43 (Santa Cruz Biotechnology). The immunogen is identical to corresponding mouse sequence (Procacci et al., 2008).

The Na+/K+-ATPase antibody (Santa Cruz Biotechnology, Cat# sc-28800, RRID: AB_2290063) recognized multiple bands between 100 and 113 kDa, corresponding to the α1 isoform, on Western blots of non-transfected 293T, human Na^+/K^+-ATPase α1 transfected 293T, and HeLa whole cell lysates (Santa Cruz Biotechnology). As expected, immunofluorescence staining of frozen mouse heart sections was localized to the cell membranes (Santa Cruz Biotechnology).

The rabbit anti-ZO-1 antibody (Thermo Fisher Scientific, Cat# 40–2200, RRID: AB_10104693) recognized a single band of 225 kD molecular weight on western blot of MDCKII, A431, Caco-2, Rat-1, NRK-52E cell lysates. In immunofluorescence staining of MDCKII cells, mouse brain mossy fiber terminals, and blood vessels of mouse heart tissue, staining was localized to the cell membranes as expected (Thermo Fisher Scientific).

The polyclonal goat anti-Otx2 (R and D Systems, Cat# AF1979, RRID: AB_2157172; JCN antibody data base #5028) was raised in immunized goats against the human Otx2 (aa 1–289) made in *E. coli*. The antibody was purified by affinity chromatography and the specificity was confirmed by nuclear immunostaining on human NTERA-2 cells (R and D Systems). We confirmed the specificity of antibody by comparison of the labeling patterns obtained by immunocytochemistry and by in situ hybridization.

The P-cadherin antibody (Invitrogen, Cat# 132000Z, RRID: AB_86574; JCN antibody database #5049) recognized a single band of 118 kDa molecular weight on immunoblot analysis of PSA5-E cells in the presence of Ca^{2+}, but did not react with surface components of cells known to express other cadherins. Moreover, E-cadherin and N-cadherin specific antibodies did not react with the PSA5-E cells. The antibody was determined to recognize the protein moiety of the P-cadherin glycoprotein, as it recognized two bands, one at 118 kDa and another at 110 kDa, after cell treatment with tunicamycin. The lower molecular weight band is consistent with the mass of the unglycosylated protein (Nose and Takeichi, 1986). The specificity of antibody was determined by comparison of the labeling patterns obtained by immunocytochemistry and by in situ hybridization (Akins et al., 2007).

The MITF antibody (Thermo Scientific, Cat# MS-771-P0, RRID: AB_141540) was raised against a histidine fusion protein expressed from the amino-terminal Taq-Sac fragment of human MITF cDNA and produces a specific gel-mobility supershift with Mi, but not with the related proteins TFEB, TFEC, and TFE3(Hemesath et al., 1998). We confirmed the specificity of antibody by comparison of the labeling patterns obtained by immunocytochemistry and by in situ hybridization.

The Vinculin antibody (Sigma-Aldrich, Cat# V9131, RRID: AB_477629) recognized a single band of 116 kDa molecular weight on Western Blot. In immunofluorescent staining of tissue and cultured cells, staining is observed at cell-cell and cell-substrate interfaces (Sigma-Aldrich).

Rabbit anti-Cx43 antibody (Sigma-Aldrich, Cat# C6219, RRID: AB_476857; JCN antibody data base #1756) recognized a single band or 2–3 bands in the vicinity of 43 kDa. This staining was specifically inhibited by the Cx43 peptide consisting of amino acid residues 363–382. Immunofluorescent staining of BHK cells and human heart sections with the

antibody showed punctate staining at cell-cell interfaces (Sigma-Aldrich). This antibody recognizes both phosphorylated and non-phosphorylated Cx43 (Matsushita et al., 2006).

In Western blot, the phospho-connexin43 (Ser368) antibody (Cell Signaling Technology, Cat# 3511S, RRID: AB_2110169) recognized a band of about 44kDa in COS and C6 cell extracts when treated with PMA, and not in the untreated cells (Cell Signaling Technology). The 44kDa band was also recognized by Western blot in rat heart extracts (Matsushita et al., 2006).

Statistical analysis

To determine statistical significance, we used the unpaired *t* test if the data followed a Gaussian distribution and showed equal standard deviations (SDs), and Welch's t test if the data followed a Gaussian distribution but showed different SDs. The Mann-Whitney test was used when the data did not follow a Gaussian distribution.

Results

RPE cell markers are expressed similarly in the albino and pigmented RPE

Otx2 and Mitf are two principal transcription factors regulating RPE specification and differentiation in the developing optic cup (Martinez-Morales et al., 2004; Bharti et al., 2006). Otx2 also acts in the adult retina to maintain RPE cell integrity and melanogenesis (Béby et al., 2010). To investigate the RPE differentiation state during the period of ipsilateral RGC neurogenesis and specification, we analyzed the expression of Otx2 and Mitf by immunohistochemistry in pigmented retina in comparison to the albino retina. At E12.5, at the early stage of RPE differentiation and initial phase of RGC neurogenesis, Otx2 (Fig. 1A, B) and Mitf (Fig. 1C,D) are expressed similarly in albino and pigmented RPE nuclei. The expression patterns of Otx2 and Mitf in the RPE layer are consistent throughout the anterior-posterior and dorsal-ventral aspects of the retina in both pigmented and albino embryos.

RGCs in the VT retina specifically express the transcription factor Zic2 between E14.5 and E17.5. The albino retina has fewer Zic2-positive RGCs compared with pigmented retina and this reduction is most evident at E15.5 (Herrera et al., 2003; Bhansali et al., 2014). Therefore, we examined whether Otx2 expression in the RPE is maintained in the albino RPE at E15.5 (Fig. 1 E–H). Otx2 protein was detected in RPE nuclei and retinal progenitor cells as previously reported (Rachel et al., 2002) in both pigmented and albino retina. The level of Otx2 expression appears reduced in pigmented RPE (Fig. 1E2) compared with albino RPE (Fig. 1F2). However, at E15.5, pigmented melanosomes (Fig. 1E1) could mask fluorescent labeling. To prevent an underestimation of expression, melanin was bleached from sections prior to immunohistochemistry (Fig. 1G1,H1). Following bleaching of both pigmented and albino sections, Otx2 expression was observed at equivalent levels of intensity in pigmented and albino RPE nuclei in the VT retina (Fig. 1G2,H2). These results suggest that RPE cell fate, based on the expression of the transcription factors Otx2 and Mitf, is maintained in the albino RPE at the time of ipsilateral RGC production and specification.

Albino RPE cells have irregular and elliptical cell morphology

We next investigated the features of RPE cell morphology in pigmented and albino embryonic retina. Differentiated RPE cells possess a uniform polygonal cell size and shape when viewed as flat mounts, but in adult albino rats, the regularly tiled matrix of RPE cells is distorted by a mixture of large and small cells (Adams et al., 2010). Whether the defects in cell dimensions seen in the mature albino rat are evident during mouse embryonic retinal development has not been investigated.

At E15.5 and E17.5, the peak and late phases of ipsilateral RGC differentiation, RPE cell borders and nuclei were visualized with antibodies against ZO-1 (a tight junction marker) and Otx2, respectively, in flat mounts of the RPE (Fig. 2A). In the pigmented RPE, cells are regularly polygonal and nuclei are positioned at regular intervals (Fig. 2B). In contrast, cells in the albino RPE are variable in size and shape and their nucleus is often placed with irregular spacing. Albino RPE cells were occasionally polynuclear (data not shown), as seen in adult albino rat RPE (Adams et al., 2010).

Cell shape features were quantified using CellProfiler software (Fig. 3). At E15.5, the average area of albino RPE cells is 13.1% greater than in pigmented RPE in VT retina. At E17.5, the average area of albino RPE cells is 8.4% greater than in pigmented RPE in DT retina, while the difference in VT retina is lost (Fig. 3B). Greater irregularity of RPE cell shape in albino retina was indicated by measurements of solidity and eccentricity. Solidity was calculated as the proportion of the object area to the area of a convex envelope. Solidity equals 1 for a solid object with no holes or an object with a concave boundary (envelope); a measure smaller than 1 indicates that the object has gaps between the perimeter of the membrane and the perimeter of the envelope (i.e. possesses an irregular boundary). In the albino RPE, solidity is less than 1 and significantly different from pigmented RPE at E17.5 (Fig. 3B). These results suggest that albino RPE cells possess irregular boundaries compared with pigmented RPE cells.

Eccentricity (e) is a measure of the roundness of RPE cells. The ratio of the distance between the foci of the ellipse and its major axis length is calculated as e = 0 for circle and 1 for a line. At E17.5, the e value for albino RPE cells is greater than that of pigmented RPE cells (VT RPE: e = 0.64 in pigmented, 0.69 in albino; DT RPE: e = 0.66 in pigmented, 0.70 in albino; Fig. 3B). Other parameters (compactness, perimeter, and form factor) were measured but for these parameters, pigmented and albino RPE were not significantly different. Thus, the differences in solidity and eccentricity indicate that albino RPE cells have a less regular boundary and a more flattened or elliptical shape compared with pigmented RPE cells.

Melanosomes are fewer in number and accumulate at the apical surface in albino RPE cells

In the normal RPE, melanin is synthesized and accumulates in organelles termed melanosomes. Previous studies have shown that the loss of the ocular albinism type 1 gene, *Oa1*, leads to the formation of macromelanosomes in the RPE and abnormal retinal development, and misrouting of RGC axons (Incerti et al., 2000; Cortese et al., 2005;

Palmisano et al., 2008; Young et al., 2008). In *Oa1* knock-out mice (*Oa1*-KO), the concentration of melanosomes on the apical aspect of RPE cells (on the neural retinal side) is first seen at E15.5 (Palmisano et al., 2008). A reduced number of melanosomes are observed in *Oa1*-KO by E18.5 (Palmisano et al., 2008). To investigate whether a reduction and displacement of melanosomes also occurs in the OCA1 ($Tyr^{c2j/c2j}$ albinos, which lack functional tyrosinase), we evaluated the number and location of melanosomes in albino and pigmented RPE during the period of RGC genesis and specification of ipsi- and contralateral RGCs, at E13.5, E16.5 and E18.5. At all of these stages, melanosomes in pigmented and albino RPE are comparable in size (Fig. 4A). However, there was a trend of reduction in the density of melanosomes in albino RPE at E13.5 (45.8% fewer melanosomes per unit area in albino than in pigmented RPE, Fig. 4B). This reduction appears more striking by E18.5 (59.7% less in albino than pigmented; Fig. 4B). The trend of reduction in melanosomes in albino RPE was first observed in only the VT region at E13.5, and then observed both in VT and DT retina by E18.5 (Fig. 4B).

Next, we calculated the distribution of melanosomes across the apical-basal axis of the RPE cells (Fig. 4C). In both pigmented and albino RPE, at all ages examined, over half of all melanosomes were observed in the apical aspect. At E16.5, the percent of apical melanosomes shows a trend toward an increase in albino RPE compared with pigmented RPE (Fig. 4C). Melanosome distribution in the DT region was essentially identical to that of the VT region (data not shown).

In addition to these abnormalities in number and distribution of melanosomes, there are additional ultrastructural abnormalities in the RPE-neural retinal interface. At this interface, where dividing retinal precursor cells contact RPE cells, electron-dense filamentous structures are observed both in pigmented and albino retina (Fig. 4A, open arrowhead). These filaments are likely similar to junctional complexes that contain gap junctions and adherent junctions observed in embryonic chick RPE (Rizzolo, 1990). In pigmented retina, these structures are aligned roughly perpendicular to the RPE-neural retinal interface. In contrast, they appear shorter in the albino retina and are less perpendicular in orientation than in pigmented retina.

Intercellular junction protein localization and distribution in the albino retina

The irregular cell morphology and melanosome displacement in albino RPE suggest that the lack of pigmentation in RPE cells is associated with a disruption of intra- and possibly also intercellular integrity of the RPE layer. The integrity of the RPE layer depends on its cellular junctions, which include adherens junctions and gap junctions. To investigate this aspect further, we analyzed expression and distribution of the junctional proteins P-cadherin and Cx43 by immunohistochemistry in pigmented and albino RPE.

At E15.5, P-cadherin outlines the membrane of pigmented RPE cells (Fig. 5A). In both sections and whole mounts of albino RPE, P-cadherin labeling is detected on the RPE cell membrane but appears more diffusely distributed compared with pigmented RPE, in both VT and DT regions of the eye (Fig. 5A, B). Merged stacks reconstructed in three dimensions by confocal microscopy more precisely demonstrate the irregular P-cadherin association with the RPE cell membrane in the albino, in contrast to the more even and tight distribution

with the cell membrane in pigmented RPE cells (Fig. 5C, D). In pigmented RPE, P-cadherin labeling is aligned in the Z-plane (Fig. 5C2). In contrast, in albino RPE, P-cadherin labeling is detected in multiple positions in Z-plane (Fig. 5D2). This altered distribution of junctional proteins could be underly the irregularity of albino RPE cell shape, and could lead to defects in cell-cell adhesion.

Gap junction-mediated cellular communication has been proposed to be a regulator of retinal development (Pearson et al., 2005; Tibber et al., 2007). In pigmented and albino rat retina, Cx43 immunofluorescence was detected at the interface of the RPE and neural retina (Tibber et al., 2007). The relative area of Cx43 labeling at postnatal day (P) 1 and P4 was estimated to be greater in the albino rat RPE compared with pigmented RPE due to larger and more numerous Cx43 particles (Tibber et al., 2007). The difference, however, was not detectable prior to E18.5 (Tibber et al., 2007). As rat RGCs are generated between E13 and E19 (Reese and Colello, 1992), these observations by Tibber et al. (2007) suggest that elevated levels of Cx43 expression in albino rat retina are observed after RGC genesis.

As was the case when staining for Otx2 previously (Fig. 1E–H), we considered the possibility that the presence of pigment in the RPE after E15.5 might mask fluorescent labeling of Cx43 and lead to underestimation of Cx43 expression level. We therefore bleached pigmented and albino retinal sections prior to immunohistochemistry for Cx43 at E13.5 and E15.5 and then quantified Cx43 expression. We defined the RPE regions of interest (ROI) corresponding to ipsilateral RGCs (Zic2-positive RGCs, VT retina, Fig. 6A) and contralateral RGCs (Islet1/2-positive RGCs, DT retina, Fig. 6E) in reference sections. RPE cells were outlined by Na^+/K^+ ATPase immunofluorescence (Fig. 6B,F).

Notably, Cx43 immunofluorescence was detected in the RPE from the peripheral retina midway toward the central retina but not in the central pole region (data not shown). In the peripheral region, Cx43 signal was detected as small particles at the interface of the RPE and the neural retina as Tibber et al. (2007) reported, and along the lateral faces of RPE cells (Fig. 6C,G). To determine whether there is a difference in Cx43 expression in the albino relative to the pigmented RPE, the sum of the intensity of Cx43 particles was calculated and indicated as expression level in the VT and DT RPE (Fig. 7A). The Cx43 expression level at E13.5 and E15.5 is similar in pigmented and albino RPE.

During the protein life cycle, Cx43 can be a hexamer called a connexon or a cluster of connexons, which form a gap junction (Solan and Lampe, 2005; 2009). Variation in the localization, size and number of Cx43-positive particles may reflect a different status of Cx43 protein during the life cycle of a gap junction. Therefore, we analyzed whether Cx43 positive particles are preferentially localized at the interface of the RPE and the neural retina (the apical region of the RPE cells). More than 60% of Cx43-positive particles in both pigmented and albino RPE are localized on the apical side facing the neural retina at E13.5 and E15.5 (Fig. 7B). Further, the average size of Cx43 particles is not different between pigmented and albino RPE, in both VT and DT regions at these two ages (Fig. 7D). However, at E15.5, the total number of particles is lower in albino RPE compared with pigmented RPE (Fig. 7C). The reduction of the total number of Cx43 particles in albino RPE is due to a significant decrease in the number of smallest particles (0.04–0.29 μm^2) in albino

RPE compared with pigmented RPE (Fig. 7E). The range, distribution, and size of Cx43-positive particles other than the smallest sized particles are similar for both albino and pigmented RPE, in both the VT and DT (not shown) peripheral retina. These results suggest that total expression level of Cx43 is similar between pigmented and albino RPE but the assembly status of Cx43 may be different.

Cx43 in albino RPE is phosphorylated

Because gap junctions are a potential route of communication between the RPE and neural retina, we next analyzed the phosphorylation state of gap junctions in the RPE as an indicator of gap junction activity state. Phosphorylation of Cx43 can affect trafficking, assembly, degradation and channel gating of gap junctions (Solan and Lampe, 2014). Specifically, phosphorylation of Cx43 on serine368 (S368) decreases gap junction communication via a reduction in unitary channel conductance (Lampe and Lau, 2000; Solan et al., 2003). We tested whether Cx43 is in a different phosphorylation state, especially at S368, in pigmented and albino RPE during the time window of ipsilateral RGC genesis, using western blot analysis (Fig. 8). Anti-Cx43 antibody recognizes both phosphorylated and non-phosphorylated forms of Cx43. As previously reported (Matsushita et al., 2006), anti-Cx43 antibody recognized two major bands in RPE extracts at E13.5 and E15.5 (Fig. 8A,B). The higher band is the phosphorylated form and the lower band the dephosphorylated form. The density of the higher band tended to be greater in albino RPE compared with pigmented RPE at E13.5 and E15.5 ($P = 0.0571$, Mann-Whitney test, $n = 4$, Fig. 8D). Labeling with an anti-Phospho-Cx43 antibody, which recognizes the phosphorylated form of Cx43 at S368 (P368-Cx43), was inconsistent at E13.5 by western blot. However, immunoblots of E15 RPE showed higher levels of P368-Cx43 in albino RPE compared with pigmented RPE ($P = 0.0286$, Mann-Whitney test, $n = 4$, Fig. 8C,E). The phosphorylated state of Cx43 in albino RPE suggests that gap junctional communication may be impaired in the albino RPE.

Discussion

Our results demonstrate that during the period of ipsilateral RGC genesis and specification, in addition to the absence of melanin, albino RPE cells have defects in their stereotypical features, including irregular cell shape, skewed melanosome localization, diffuse expression of adherens junction protein, fewer but more intense and irregular gap junction puncta, and increased phosphorylation of Cx43. Below we discuss how these defects may arise and the implications for both RPE and neural retinal development.

Albino RPE cells have irregular shapes

We found that albino RPE cells have variable cell morphology, in that the number of borders deviates from the more regular cell shape observed in pigmented RPE cells (a 5–6 sided polygon; Jiang et al., 2013). Adams et al. (2010) previously described elliptical rather than circular or cuboidal cell shapes in postnatal albino rat RPE. However, in that study, the cell shape differences in embryonic RPE, in particular, during the period of RGC neurogenesis/specification and in specific regions of the retina, were not addressed. Our study compares VT retina with DT retina, with the aim of revealing differences that could preferentially

affect VT retina during the period of ipsilateral RGC genesis in this retinal region. Although cell shape defects were not specific to VT retina, the defects in both DT and VT albino retina are evident during the critical phase of RGC specification. In agreement with Adams et al. (2010), our quantification demonstrates that albino RPE cells have higher eccentricity values, reflecting elliptical rather than circular shapes, and smaller solidity values, again, suggesting irregular shapes.

ZO-1 labeling reflects RPE cell outlines primarily at the apical surface, but does not reveal the overall shape of RPE cells, because epithelial cell junctional complexes tend to be close to the apical border of RPE cells (Sparrow et al., 2010). Our findings on irregular shape features of albino RPE cells thus may preferentially reflect the interaction between the apical surface of RPE cells and the neural retina.

In albino RPE cells, P-cadherin appears more diffusely distributed and does not appear to be confined to the cell membrane compared with P-cadherin localization in pigmented RPE cells. In Z-stacks of confocal images of albino RPE cells, P-cadherin immunostaining also appears more diffusely distributed in X-Y plane but also in the Z-plane. P-cadherin may in fact be associated with the cell membrane of albino RPE cells, but because albino RPE cells are more irregular in shape, P-cadherin immunostaining in whole mount, reveals a meshwork. P-cadherin is a calcium dependent cell adhesion molecule normally localized to the RPE cell membrane. In the mouse retina, P-cadherin expression is clearly observed in pigmented RPE cells by E12.5 (Xu et al., 2002). In the pigmented RPE, calcium accumulates beginning with the appearance of pigment at E11; however, calcium accumulation is not observed in the albino mouse retina (Dräger, 1985b). These studies suggest that the emergence of pigment in the RPE may affect the distribution of P-cadherin, which in turn could lead to altered cell morphology. To address when in development these changes are initiated, morphological analyses should be carried out at the start of RPE development (E9-E13). However, dissecting and flat-mounting the RPE at such early stages is technically difficult because of the fragility of retinal tissue.

Jiang et al. (2013) hypothesized that RPE morphology changes with age and disease progression, with the extent and types of alterations depending on the disease (Jiang et al., 2013). In Rd10 mice, an autosomal recessive retinitis pigmentosa model, rod and cone photoreceptor cells degenerate, and RPE cells in Rd10 have elongated shapes compared with wild type at P100 (Jiang et al., 2013). Further analysis is needed as to whether the extent and types of changes in RPE cell shape are common to different types of albinism and to other eye diseases, especially during development.

Melanosome number and distribution are affected in the albino RPE

Our study shows that genes required in RPE cell differentiation, such as Otx2 and Mitf, are expressed similarly in albino and pigmented RPE during RGC genesis (E12.5 and E15.5). In contrast, melanosomes tend to be reduced in number in the albino, primarily at the apical side of the RPE as seen at E16.5. Previous studies suggested that Otx2 is required to maintain RPE cell integrity in adult retina (Béby et al., 2010). Specifically, Otx2 deletion in adult mouse retina causes cellular and functional alterations of RPE, including decreased *tyrosinase* mRNA, reduction of melanosomes, accumulation of residual melanosomes at the

apical side of RPE cells, and extensive vacuolization of RPE cells (Béby et al., 2010). Our results show that Otx2 expression is maintained in the RPE of the *OCA* mutant studied here in the absence of functional tyrosinase. In agreement with Béby et al. (2010), the cellular alterations we observe in the embryonic *OCA* mutant RPE are similar to those in Otx2 deleted retinae in adulthood. Our results support the view that tyrosinase is downstream of Otx2, and that functional tyrosinase and pigment accumulation are direct regulators of melanosome status in RPE cells in both developing and mature retina.

Alterations of melanosome growth and maturation have been described in the RPE of *Oa1* mutants (Incerti et al., 2000; Cortese et al., 2005; Palmisano et al., 2008; Young et al., 2008). *Oa1* encodes a 404-amino acid protein, which has homology with members of the G-protein coupled receptor family, and in its absence, melanosomes are reduced, greatly enlarged due to aberrant turnover, and located more apically than in wild type RPE cells. Palmisano et al. (2008), suggest that the abnormal organelle distribution might represent an early event in the pathogenesis of the retinal abnormalities in albino animals. Our findings on OCA RPE that melanosomes are reduced is in agreement with a reduced melanosome number in *Oa1* mutants except for melanosome size, which seems to be unchanged in OCA RPE. In addition, we find that the reduction of melanosomes becomes evident first in VT retina, where ipsilateral RGCs are located, and only later in both VT and DT retina. Importantly, both OCA and OA1 have scant melanin content and fewer ipsilateral RGCs, although the final common pathway in these two genotypes that leads to a reduced ipsilateral projection is still not understood.

Junctional protein-mediated cell-cell communication between RPE and neural retina

Cx43 is a major gap junction protein expressed in RPE cells of many vertebrates (Janssen-Bienhold et al., 1998). In previous studies on the albino rat RPE, Cx43 was not detected at E15.5 and while Cx43 expression was evident at E18.5, it was not reported to be different in pigmented and albino RPE (Tibber et al., 2007). At later postnatal ages, greater Cx43 expression in the albino RPE was thought to be due to more large Cx43 particles compared with pigmented RPE (Tibber et al., 2007). However, these data were not quantified. Our results show that Cx43 is detectable in the embryonic mouse eye during RGC genesis and specification of ipsi- and contralateral RGCs (E13.5 and E15.5). Fewer Cx43 particles are observed in albino RPE, although the average particle size is similar in embryonic albino and pigmented RPE. The discrepancies between our findings and those of Tibber et al. (2007) could be due to melanosome pigment masking fluorescent protein signals in pigmented RPE. Our melanin bleaching procedure allows more precise detection of Cx43 expression and more accurate comparison between genotypes.

Antibody specificity could also account for the differences in our findings on Cx43 expression and those of Tibber et al. (2007). Tibber et al. (2007) used an antibody that recognizes both phosphorylated and unphosphorylated Cx43. The antibody used for immunofluorescence in the present Figure 6 recognizes unphosphorylated Cx43 according to the manufacturer (Santa Cruz). Quantification of our western blots (Fig. 8D) showed that the intensity of unphosphorylated Cx43 is similar in pigmented and albino RPE samples (Fig. 8D, bottom bands), agreeing with our quantification of Cx43 expression levels by

immunohistochemistry (Fig. 7A). Cx43 staining (Fig. 6D) could appear to have greater intensity in the albino compared with pigmented retina because there are fewer small particles in the albino, but a similar number of large particles (Fig.7 D , E), giving the illusion of a greater level of fluorescence in the albino retina.

Cx43 protein localization reflects several stages of the connexon life cycle, including trafficking and degradative states, both of which are intracellular. The assembled state occurs on the cell membrane. Our data shows that Cx43 particle number primarily of the smallest detectable particles is reduced in the albino RPE. Cx43 oligomerizes into connexons that are transported to the cell surface (Solan and Lampe, 2005; 2009). Assembling a cluster of connexons with connexon counterparts from an apposing cell leads to the formation of a mature gap junction. Unassembled connexons (hemichannels) in extra-junctional regions of the cell membrane can also signal (Cook and Becker 2009). Fewer smaller particles of Cx43 could be due to a). a reduced pool of connexins, several of which form a connexon, and in turn, fewer anchored gap-junctional plaques; or b). a reduced number of free-floating Cx43 hemichannels that would change the balance of different connexin-based signaling pathways. The specific stage of the Cx43 life cycle affected in the albino RPE remains to be elucidated.

Our study is the first to describe phosphorylation of Cx43 on serine 368 in the albino RPE compared with pigmented RPE. In rat epithelial cells, phosphorylation of Cx43 on serine 368 reduces gap junction communication by alteration of channel conductance (Lampe and Lau, 2000; Solan et al., 2003). Our data on increased phosphorylation of Cx43 on serine 368 in albino RPE thus implicates impaired gap junction communication in the albino mouse retina during RGC genesis at E15.5. This is especially intriguing in light of our previous studies demonstrating alterations in RGC neurogenesis in the albino mouse retina (Rachel et al., 2002), e.g., fewer Zic2-positive RGCs are born at E13.5-E14.5 and a delay in the peak of neurogenesis of ipsilateral RGCs (Bhansali et al., 2014). L-Dopa is synthesized and accumulates in the pigmented mouse RPE starting at E10.5, but is missing in the albino mouse (Roffler-Tarlov et al., 2013). L-Dopa is an intermediate product of the melanin synthesis pathway and has been proposed to be a mitotic regulator in the pigmented and albino rat retina (Ilia and Jeffery, 1999). L-Dopa injection into the albino rat retina at postnatal ages elevates the rate of mitosis in the neural retina (Tibber et al., 2007). In addition, in chick retina, gap junction hemichannel-mediated ATP release from RPE cells to the neural retina accelerates cell division and proliferation in the neural retina (Pearson et al., 2005). It is possible that reduced gap junction communication via Cx43 pS368 or reduced signaling via gap-junction-channel independent but connexin protein dependent junctions, i.e. hemichannels (unassembled connexons) in the albino RPE causes a reduction in the release of a pro-cell division signal, such as ATP and/or L-Dopa, from the RPE to the neural retina. This reduction in turn would lead to a shift in the timing of neurogenesis of RGCs in the albino retina that would result in a reduction of the ipsilateral RGC population. Although the defects of albino RPE cell integrity presented here are not VT retina-specific, expression of a receptor for a putative RPE derived signal might affect retinal precursors in VT retina that become ipsilateral RGCs.

How do defects in the albino RPE stem from an absence of melanin?

Melanin regulates Ca^{2+} homeostasis in melanocytes (Bush and Simon, 2007). In the RPE, Ca^{2+} accumulation has been detected in pigmented but not in the albino retina (Dräger, 1985b). One hypothesis is that the lack of melanin changes the concentration of Ca^{2+}. In addition to altering the arrangement of P-cadherin and cytoskeletal elements, which influences melanosome distribution (Futter et al., 2004; Palmisano et al., 2008), disruption of epithelial junctional protein complexes is likely to affect Cx43 hemichannel signaling (Evans et al., 2006; Cook and Becker, 2009). In addition, changes in intracellular Ca^{2+} could mediate channel gating of gap junctions (Bukauskas and Verselis, 2004).

The absence of melanin could also lead to perturbations in the formation of junctional complexes. As in other epithelial cells, the assembly of junctional complexes (tight, adherens and gap junctions) affects the definition and, ultimately, the maintenance of RPE cell polarity (Stein et al., 2002; Sparrow et al., 2010). The establishment of proper cell polarity with apical and basolateral plasma membrane domains ensures accurate intracellular trafficking directing domain-specific targeting of molecules. In the RPE, proteins enriched in apical or basal regions of the cells are important for controlling ion concentration and secretion of molecules from the RPE. Mutations in polarized proteins in RPE, such as bestrophin and the c-mer tyrosine kinase receptor, are associated with retinal degeneration, e.g., Best vitelliform macular dystrophy and retinitis pigmentosa, respectively (Sparrow et al., 2010).

In sum, we have demonstrated a number of cellular perturbations in the albino RPE that point to perturbed cell integrity relevant to cell-cell communication. These perturbations include aberrant cell shape, altered localization of melanosomes, altered phosphorylation of gap junctional protein, and possible defects in gap junction assembly. Such defects could affect the maintenance of RPE integrity as well as polarized secretion of factors to the developing neural retina to regulate ipsilateral RGC specification during RGC neurogenesis.

Acknowledgments

We thank members of the Mason laboratory and Drs. Takeshi Sakurai and Janet Sparrow for helpful discussions and for critical reading of the manuscript. We also thank Drs. Theresa Swayne and Laura Munteanu (Confocal and Specialized Microscopy Core at the Herbert Irving Comprehensive Cancer Center, Columbia University Medical Center) for assistance with imaging.

Grant information: NIH grants R01 EY012736, R21 EY023714 (CM), and Fight for Sight, Uehara Memorial Foundation, Daiichi Sankyo Foundation, and Hayashi Memorial Foundation (LI)

Literature Cited

Adams T, Shahabi G, Hoh-Kam J, Jeffery G. Held under arrest: Many mature albino RPE cells display polyploidal features consistent with abnormal cell cycle retention. Experimental eye research. 2010; 90(2):368–372. [PubMed: 19833124]

Akins MR, Benson DL, Greer CA. Cadherin expression in the developing mouse olfactory system. J Comp Neurol. 2007; 501(4):483–497. [PubMed: 17278136]

Badea TC, Nathans J. Morphologies of mouse retinal ganglion cells expressing transcription factors Brn3a, Brn3b, and Brn3c: analysis of wild type and mutant cells using genetically-directed sparse labeling. Vision Res. 2011; 51(2):269–279. [PubMed: 20826176]

Béby F, Housset M, Fossat N, Le Greneur C, Flamant F, Godement P, Lamonerie T. Otx2 gene deletion in adult mouse retina induces rapid RPE dystrophy and slow photoreceptor degeneration. PloS one. 2010; 5(7):e11673. [PubMed: 20657788]

Bertolotti E, Neri A, Camparini M, Macaluso C, Marigo V. Stem cells as source for retinal pigment epithelium transplantation. Progress in retinal and eye research. 2014; 42:130–144. [PubMed: 24933042]

Bhansali P, Rayport I, Rebsam A, Mason C. Delayed neurogenesis leads to altered specification of ventrotemporal retinal ganglion cells in albino mice. Neural development. 2014; 9:11. [PubMed: 24885435]

Bharti K, Nguyen MTT, Skuntz S, Bertuzzi S, Arnheiter H. The other pigment cell: specification and development of the pigmented epithelium of the vertebrate eye. Pigment cell research. 2006; 19(5): 380–394. [PubMed: 16965267]

Bodenstein L, Sidman RL. Growth and development of the mouse retinal pigment epithelium. I. Cell and tissue morphometrics and topography of mitotic activity. Dev Biol. 1987; 121(1):192–204. [PubMed: 3569658]

Brown LY, Kottmann AH, Brown S. Immunolocalization of Zic2 expression in the developing mouse forebrain. Gene Expr Patterns. 2003; 3(3):361–367. [PubMed: 12799086]

Bukauskas FF, Verselis VK. Gap junction channel gating. Biochim Biophys Acta. 2004; 1662(1–2): 42–60. [PubMed: 15033578]

Bush WD, Simon JD. Quantification of Ca(2+) binding to melanin supports the hypothesis that melanosomes serve a functional role in regulating calcium homeostasis. Pigment Cell Res. 2007; 20(2):134–139. [PubMed: 17371440]

Cook JE, Becker DL. Gap-junction proteins in retinal development: new roles for the "nexus". Physiology (Bethesda). 2009; 24:219–230. [PubMed: 19675353]

Cortese K, Giordano F, Surace EM, Venturi C, Ballabio A, Tacchetti C, Marigo V. The ocular albinism type 1 (OA1) gene controls melanosome maturation and size. Investigative ophthalmology & visual science. 2005; 46(12):4358–4364. [PubMed: 16303920]

Dräger UC. Birth dates of retinal ganglion cells giving rise to the crossed and uncrossed optic projections in the mouse. Proceedings of the Royal society of London Series B Biological sciences. 1985a; 224(1234):57–77.

Dräger UC. Calcium binding in pigmented and albino eyes. Proc Natl Acad Sci U S A. 1985b; 82(19): 6716–6720. [PubMed: 3863122]

Erskine L, Herrera E. Connecting the retina to the brain. ASN Neuro. 2014; 6(6)

Erskine L, Reijntjes S, Pratt T, Denti L, Schwarz Q, Vieira JM, Alakakone B, Shewan D, Ruhrberg C. VEGF signaling through neuropilin 1 guides commissural axon crossing at the optic chiasm. Neuron. 2011; 70(5):951–965. [PubMed: 21658587]

Evans WH, De Vuyst E, Leybaert L. The gap junction cellular internet: connexin hemichannels enter the signalling limelight. Biochem J. 2006; 397(1):1–14. [PubMed: 16761954]

Foss AJ, Alexander RA, Jefferies LW, Lightman S. Immunohistochemical techniques: the effect of melanin bleaching. Br J Biomed Sci. 1995; 52(1):22–25. [PubMed: 7549602]

Fuhrmann S, Zou C, Levine EM. Retinal pigment epithelium development, plasticity, and tissue homeostasis. Experimental eye research. 2014; 123:141–150. [PubMed: 24060344]

Futter CE, Ramalho JS, Jaissle GB, Seeliger MW, Seabra MC. The role of Rab27a in the regulation of melanosome distribution within retinal pigment epithelial cells. Mol Biol Cell. 2004; 15(5):2264–2275. [PubMed: 14978221]

Giordano F, Bonetti C, Surace EM, Marigo V, Raposo G. The ocular albinism type 1 (OA1) G-protein-coupled receptor functions with MART-1 at early stages of melanogenesis to control melanosome identity and composition. Human Molecular Genetics. 2009; 18(23):4530–4545. [PubMed: 19717472]

Hemesath TJ, Price ER, Takemoto C, Badalian T, Fisher DE. MAP kinase links the transcription factor Microphthalmia to c-Kit signalling in melanocytes. Nature. 1998; 391(6664):298–301. [PubMed: 9440696]

Herrera E, Brown L, Aruga J, Rachel RA, Dolen G, Mikoshiba K, Brown S, Mason CA. Zic2 patterns binocular vision by specifying the uncrossed retinal projection. Cell. 2003; 114(5):545–557. [PubMed: 13678579]

Ilia M, Jeffery G. Retinal mitosis is regulated by dopa, a melanin precursor that may influence the time at which cells exit the cell cycle: analysis of patterns of cell production in pigmented and albino retinae. The Journal of comparative neurology. 1999; 405(3):394–405. [PubMed: 10076934]

Incerti B, Cortese K, Pizzigoni A, Surace EM, Varani S, Coppola M, Jeffery G, Seeliger M, Jaissle G, Bennett DC, Marigo V, Schiaffino MV, Tacchetti C, Ballabio A. Oa1 knock-out: new insights on the pathogenesis of ocular albinism type 1. Human Molecular Genetics. 2000; 9(19):2781–2788. [PubMed: 11092754]

Janssen-Bienhold U, Dermietzel R, Weiler R. Distribution of connexin43 immunoreactivity in the retinas of different vertebrates. J Comp Neurol. 1998; 396(3):310–321. [PubMed: 9624586]

Jeffery G. The retinal pigment epithelium as a developmental regulator of the neural retina. Eye. 1998; 12:499–503. [PubMed: 9775209]

Jiang Y, Qi X, Chrenek MA, Gardner C, Boatright JH, Grossniklaus HE, Nickerson JM. Functional principal component analysis reveals discriminating categories of retinal pigment epithelial morphology in mice. Investigative ophthalmology & visual science. 2013; 54(12):7274–7283. [PubMed: 24114543]

Karlsson O, Thor S, Norberg T, Ohlsson H, Edlund T. Insulin gene enhancer binding protein Isl-1 is a member of a novel class of proteins containing both a homeo- and a Cys-His domain. Nature. 1990; 344(6269):879–882. [PubMed: 1691825]

Kuwabara T, Weidman TA. Development of the prenatal rat retina. Invest Ophthalmol. 1974; 13(10): 725–739. [PubMed: 4412789]

Kuwajima T, Yoshida Y, Takegahara N, Petros TJ, Kumanogoh A, Jessell TM, Sakurai T, Mason C. Optic chiasm presentation of Semaphorin6D in the context of Plexin-A1 and Nr-CAM promotes retinal axon midline crossing. Neuron. 2012; 74(4):676–690. [PubMed: 22632726]

Lampe PD, Lau AF. Regulation of gap junctions by phosphorylation of connexins. Arch Biochem Biophys. 2000; 384(2):205–215. [PubMed: 11368307]

Martinez-Morales J, Rodrigo I, Bovolenta P. Eye development: a view from the retina pigmented epithelium. Bioessays. 2004; 26(7):766–777. [PubMed: 15221858]

Matsushita S, Kurihara H, Watanabe M, Okada T, Sakai T, Amano A. Alterations of phosphorylation state of connexin 43 during hypoxia and reoxygenation are associated with cardiac function. J Histochem Cytochem. 2006; 54(3):343–353. [PubMed: 16314445]

Nose A, Takeichi M. A novel cadherin cell adhesion molecule: its expression patterns associated with implantation and organogenesis of mouse embryos. J Cell Biol. 1986; 103(6 Pt 2):2649–2658. [PubMed: 3539943]

Orchard GE, Calonje E. The effect of melanin bleaching on immunohistochemical staining in heavily pigmented melanocytic neoplasms. Am J Dermatopathol. 1998; 20(4):357–361. [PubMed: 9700373]

Pak W, Hindges R, Lim YS, Pfaff SL, O'Leary DD. Magnitude of binocular vision controlled by islet-2 repression of a genetic program that specifies laterality of retinal axon pathfinding. Cell. 2004; 119(4):567–578. [PubMed: 15537545]

Palmisano I, Bagnato P, Palmigiano A, Innamorati G, Rotondo G, Altimare D, Venturi C, Sviderskaya EV, Piccirillo R, Coppola M, Marigo V, Incerti B, Ballabio A, Surace EM, Tacchetti C, Bennett DC, Schiaffino MV. The ocular albinism type 1 protein, an intracellular G protein-coupled receptor, regulates melanosome transport in pigment cells. Human Molecular Genetics. 2008; 17(22):3487–3501. [PubMed: 18697795]

Pearson RA, Dale N, Llaudet E, Mobbs P. ATP released via gap junction hemichannels from the pigment epithelium regulates neural retinal progenitor proliferation. Neuron. 2005; 46(5):731–744. [PubMed: 15924860]

Perron JC, Dodd J. ActRIIA and BMPRII Type II BMP receptor subunits selectively required for Smad4-independent BMP7-evoked chemotaxis. PloS one. 2009; 4(12):e8198. [PubMed: 20011660]

Petros TJ, Rebsam A, Mason CA. Retinal axon growth at the optic chiasm: to cross or not to cross. Annu Rev Neurosci. 2008; 31:295–315. [PubMed: 18558857]

Procacci P, Magnaghi V, Pannese E. Perineuronal satellite cells in mouse spinal ganglia express the gap junction protein connexin43 throughout life with decline in old age. Brain research bulletin. 2008; 75(5):562–569. [PubMed: 18355632]

Rachel RA, Dolen G, Hayes NL, Lu A, Erskine L, Nowakowski RS, Mason CA. Spatiotemporal features of early neuronogenesis differ in wild-type and albino mouse retina. The Journal of neuroscience. 2002; 22(11):4249–4263. [PubMed: 12040030]

Raymond SM, Jackson IJ. The retinal pigmented epithelium is required for development and maintenance of the mouse neural retina. Curr Biol. 1995; 5(11):1286–1295. [PubMed: 8574586]

Rebsam A, Bhansali P, Mason CA. Eye-Specific Projections of Retinogeniculate Axons Are Altered in Albino Mice. The Journal of neuroscience. 2012; 32(14):4821–4826. [PubMed: 22492037]

Reese BE, Colello RJ. Neurogenesis in the retinal ganglion cell layer of the rat. Neuroscience. 1992; 46(2):419–429. [PubMed: 1542415]

Rizzolo LJ. The distribution of Na+,K(+)-ATPase in the retinal pigmented epithelium from chicken embryo is polarized in vivo but not in primary cell culture. Experimental eye research. 1990; 51(4):435–446. [PubMed: 2170160]

Roffler-Tarlov S, Liu JH, Naumova EN, Bernal-Ayala MM, Mason CA. L-Dopa and the albino riddle: content of L-Dopa in the developing retina of pigmented and albino mice. PloS one. 2013; 8(3):e57184. [PubMed: 23526936]

Solan JL, Fry MD, TenBroek EM, Lampe PD. Connexin43 phosphorylation at S368 is acute during S and G2/M and in response to protein kinase C activation. J Cell Sci. 2003; 116(Pt 11):2203–2211. [PubMed: 12697837]

Solan JL, Lampe PD. Connexin phosphorylation as a regulatory event linked to gap junction channel assembly. Biochim Biophys Acta. 2005; 1711(2):154–163. [PubMed: 15955300]

Solan JL, Lampe PD. Connexin43 phosphorylation: structural changes and biological effects. Biochem J. 2009; 419(2):261–272. [PubMed: 19309313]

Solan JL, Lampe PD. Specific Cx43 phosphorylation events regulate gap junction turnover in vivo. FEBS Lett. 2014; 588(8):1423–1429. [PubMed: 24508467]

Sparrow JR, Hicks D, Hamel CP. The retinal pigment epithelium in health and disease. Curr Mol Med. 2010; 10(9):802–823. [PubMed: 21091424]

Stein M, Wandinger-Ness A, Roitbak T. Altered trafficking and epithelial cell polarity in disease. Trends Cell Biol. 2002; 12(8):374–381. [PubMed: 12191914]

Thor S, Ericson J, Brannstrom T, Edlund T. The homeodomain LIM protein Isl-1 is expressed in subsets of neurons and endocrine cells in the adult rat. Neuron. 1991; 7(6):881–889. [PubMed: 1764243]

Tibber MS, Becker D, Jeffery G. Levels of transient gap junctions between the retinal pigment epithelium and the neuroblastic retina are influenced by catecholamines and correlate with patterns of cell production. The Journal of comparative neurology. 2007; 503(1):128–134. [PubMed: 17480016]

Tsuchida T, Ensini M, Morton SB, Baldassare M, Edlund T, Jessell TM, Pfaff SL. Topographic organization of embryonic motor neurons defined by expression of LIM homeobox genes. Cell. 1994; 79(6):957–970. [PubMed: 7528105]

Williams SE, Grumet M, Colman DR, Henkemeyer M, Mason CA, Sakurai T. A role for Nr-CAM in the patterning of binocular visual pathways. Neuron. 2006; 50(4):535–547. [PubMed: 16701205]

Williams SE, Mann F, Erskine L, Sakurai T, Wei S, Rossi DJ, Gale NW, Holt CE, Mason CA, Henkemeyer M. Ephrin-B2 and EphB1 mediate retinal axon divergence at the optic chiasm. Neuron. 2003; 39(6):919–935. [PubMed: 12971893]

Xu L, Overbeek PA, Reneker LW. Systematic analysis of E-, N-and P-cadherin expression in mouse eye development. Experimental eye research. 2002; 74(6):753–760. [PubMed: 12126948]

Young A, Powelson EB, Whitney IE, Raven MA, Nusinowitz S, Jiang M, Birnbaumer L, Reese BE, Farber DB. Involvement of OA1, an intracellular GPCR, and G alpha i3, its binding protein, in melanosomal biogenesis and optic pathway formation. Investigative ophthalmology & visual science. 2008; 49(7):3245–3252. [PubMed: 18378571]

In albinism, ipsilateral retinal ganglion cells (RGCs) are reduced. To dissect how melanin affects visual pathway development, we compared embryonic albino and pigmented retinal pigment epithelium (RPE). The perturbations of albino RPE cells charted here could affect RPE integrity and communication with neural precursors during RGC differentiation and axon projection.

IHC, P-cadherin, RPE wholemount, E15.5

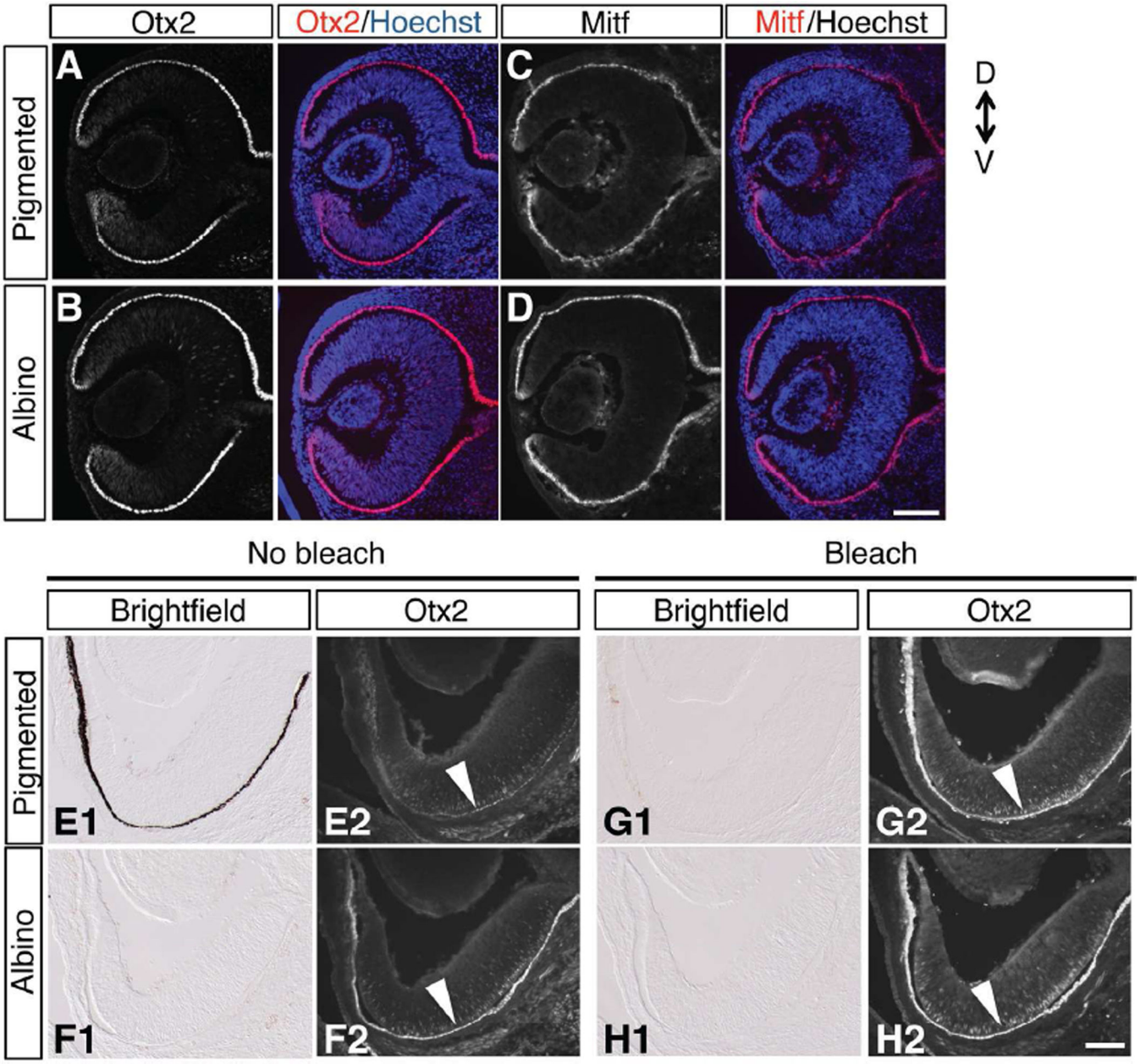

Figure 1. Markers of differentiated RPE, Otx2 and Mitf, are expressed similarly in both pigmented and albino RPE

A–D: Frontal sections of temporal retina immunostained with antibodies against Otx2 (**A, B**) and Mitf (**C, D**) at E12.5. **E-H**: Frontal sections of ventrotemporal (VT) retina at E15.5, showing that pigment accumulation in the pigmented RPE (**E1**) masks immunofluorescence of Otx2 in pigmented retina (**E2**) compared with albino retina (**F2**). Bleaching prior to immunohistochemistry (**G1, G2, H1, H2**) preserves retinal structure and shows that Otx2 is expressed in both pigmented (**G2**) and albino RPE (**H2**) at relatively equivalent levels. Scale bars: 100 μm. D, dorsal; V, ventral.

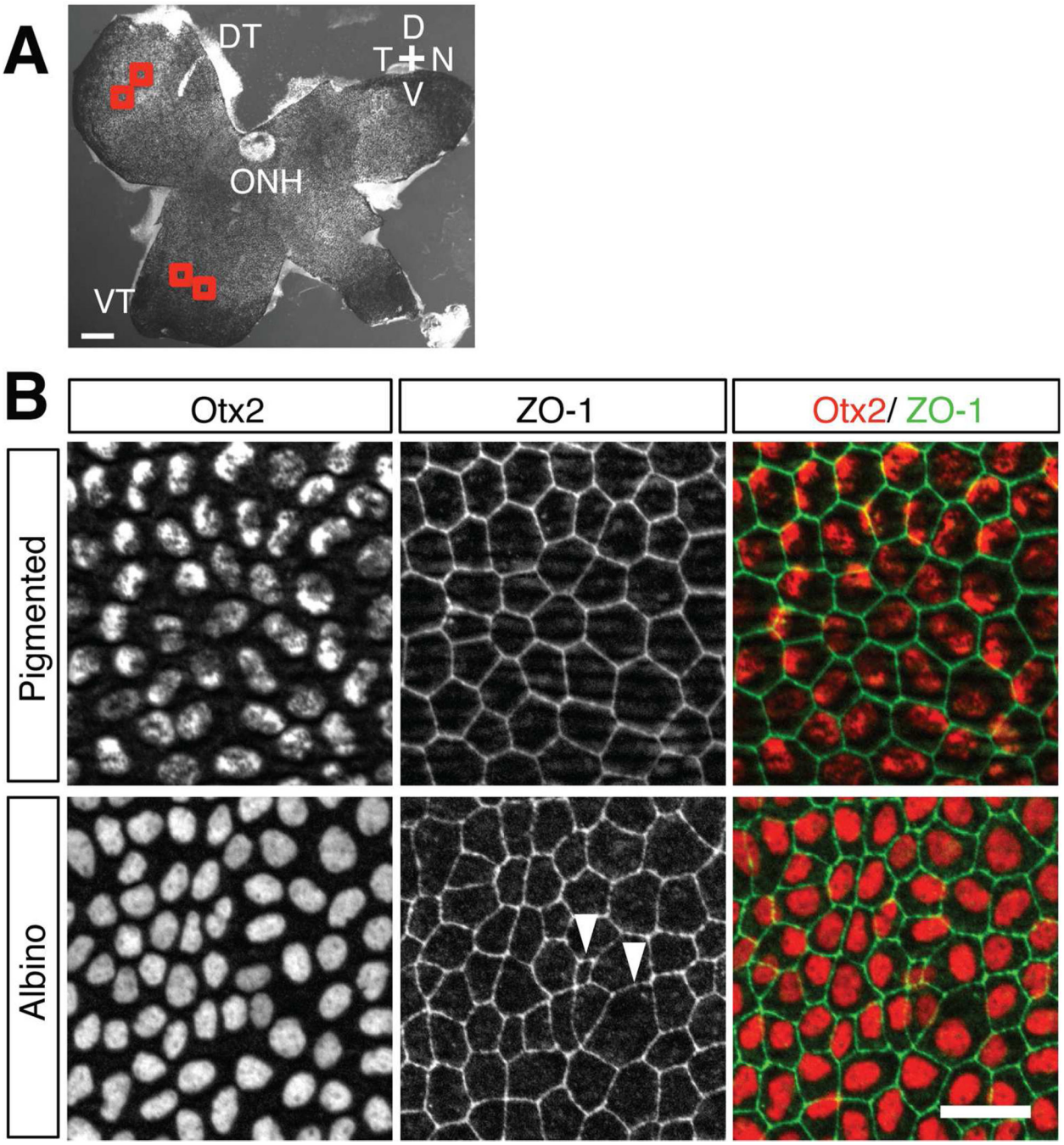

Figure 2. Cell morphology in the albino RPE is more variable than in pigmented RPE at E15.5

A: Whole-RPE flatmount of a pigmented mouse retina. Two regions from the same quadrant (in the dorsotemporal, DT, or ventrotemporal, VT, quadrant) of the RPE were selected as regions of interest for quantification of cell area and shape (red boxes). ONH, optic nerve head; D, dorsal; N, nasal; T, temporal; V, ventral. **B**: Higher magnification of the VT region in an RPE flatmount at E15.5. RPE nuclei were stained with anti-Otx2 (red) and RPE cell boundaries were stained with anti-ZO-1 (green). In pigmented RPE, cells have regular shapes and sizes, while in albino RPE, cell shape and size are variable (arrowheads). Note

that the pattern of Otx2 distribution in the nuclei appears spotty due to overlap with pigmented melanosomes. Scale bars: 200 μm (A), 25 μm (B).

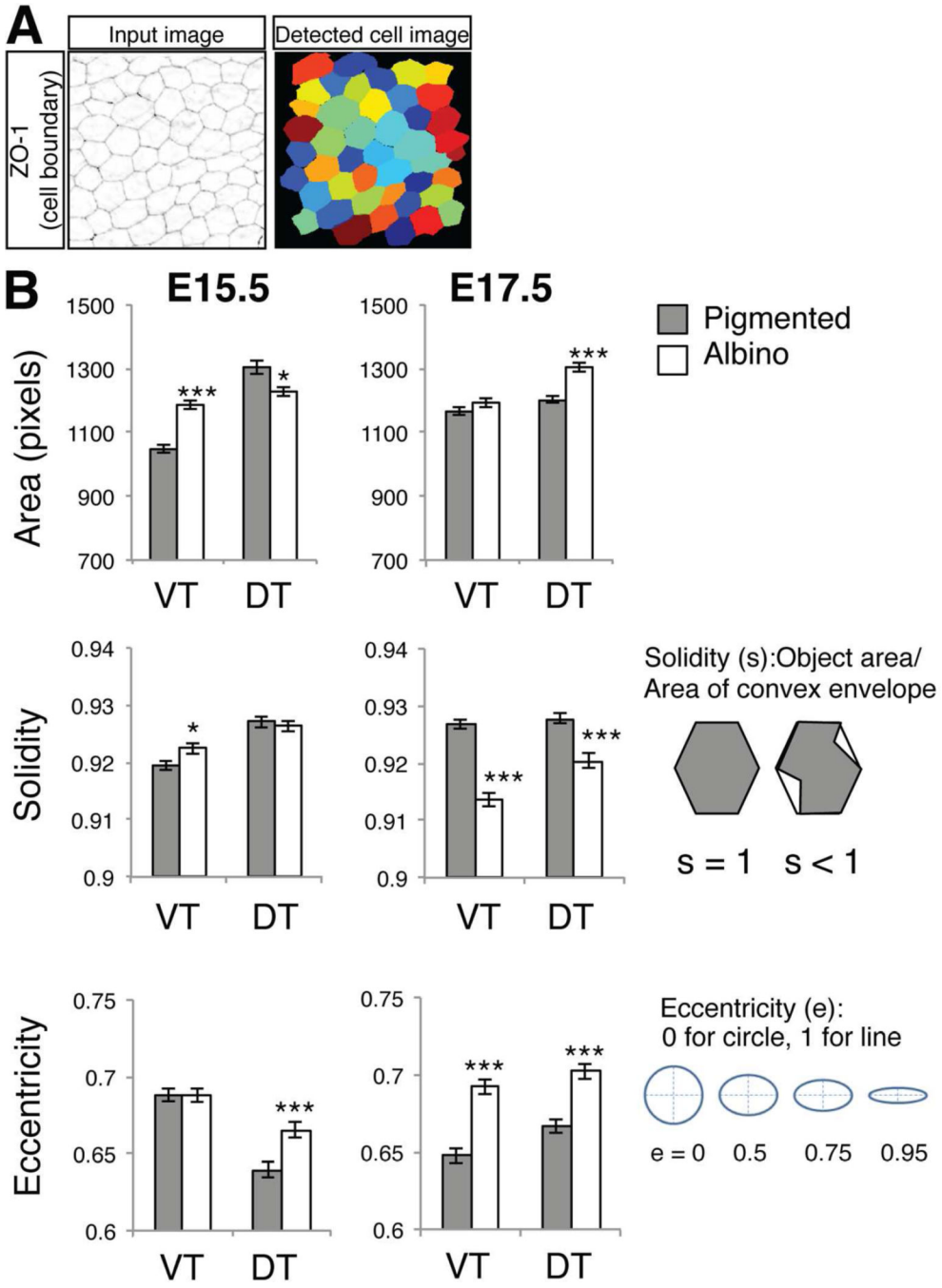

Figure 3. Comparison of cell shape in pigmented and albino RPE at E15.5 and E17.5

A: Quantification of RPE cell area and shape parameters by CellProfiler. Background noise was subtracted and ZO-1 (RPE cell boundary) signals were processed by CellProfiler (Input Image). Detected individual cells (Detected cell image) were analyzed by cell shape parameters. **B**: Measures of area and cell shape factors (solidity and eccentricity) of individual RPE cells. Area is defined by the number of pixels in a RPE cell. Solidity is the proportion of the object area (RPE cell) that fills a convex box conscribed around the object (cell). Solidity = 1 is for a solid object with no holes or concave boundary; solidity < 1 for

an object with holes or an irregular boundary. Eccentricity is the ratio of the distance between the foci of the ellipse and it's the length of its major axis. Eccentricity of 0 is a circle and 1 is a line. Bars represent mean (± SEM). *$P < 0.05$, **$P < 0.01$, ***$P < 0.001$ by Mann-Whitney test (actual P values: area E15.5 VT $P < 0.0001$, DT $P = 0.04$, E17.5 VT $P = 0.3678$, DT $P < 0.0001$. Solidity E15.5 VT $P = 0.0163$, DT $P = 0.6181$, E17.5 VT $P < 0.0001$, DT $P = 0.0002$. Eccentricity E15.5 VT $P = 0.9153$, DT, $P = 0.0004$, E17.5 VT $P < 0.0001$, DT $P < 0.0001$). Number of embryos analyzed for cell shape analysis: 8 (E15.5 pigmented VT), 9 (E15.5 albino VT), 7 (E15.5 pigmented DT), 8 (E15.5 albino DT), 8 (E17.5 pigmented and albino VT and DT). Total number of RPE cells analyzed: pigmented = 1707, albino = 1809 at E15.5; pigmented = 1838, albino = 1703 at E17.5.

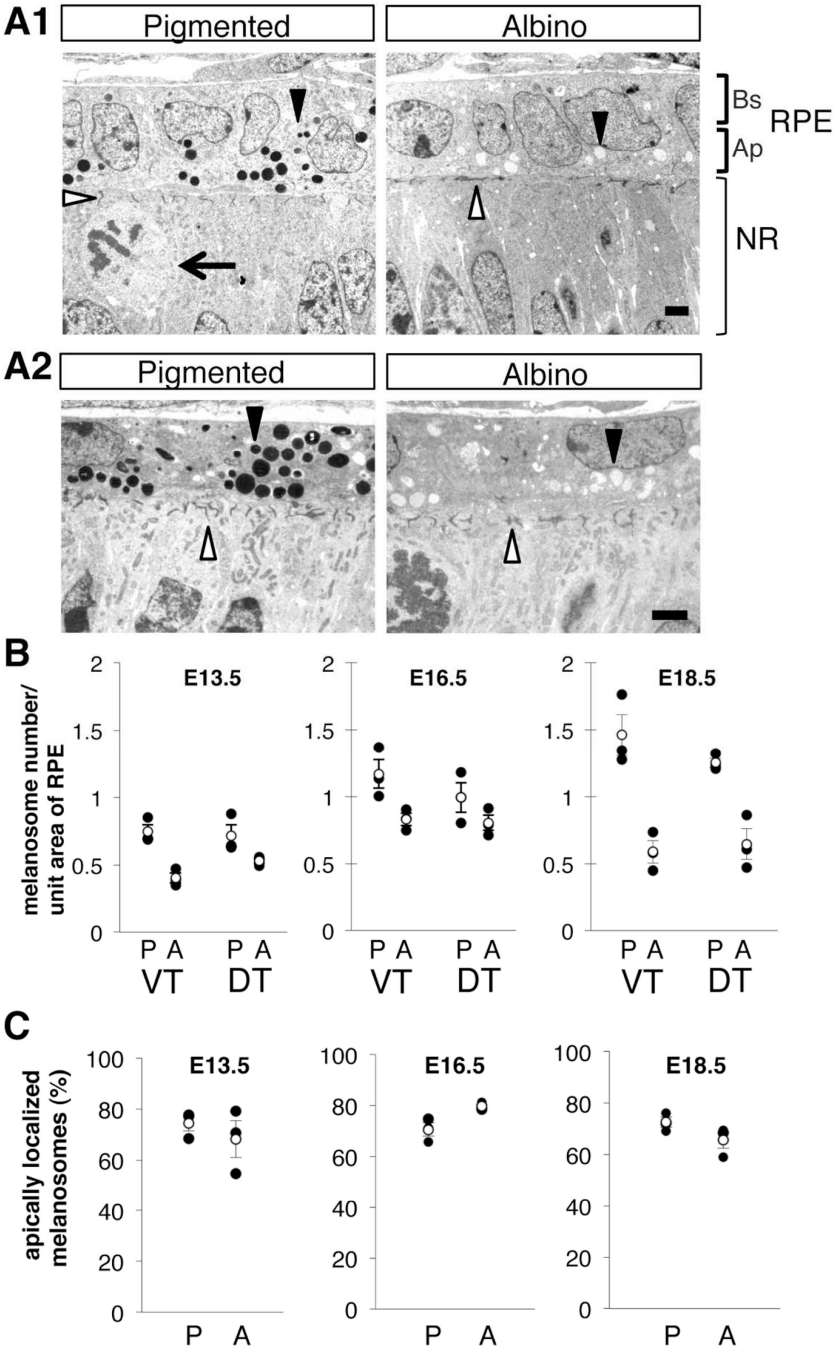

Figure 4. Melanosomes are reduced in number and concentrated apically in albino RPE cells

A: Ultrastructure of RPE cells in the VT region from pigmented and albino mice at E13.5 (**A1**) and E16.5 (**A2**). In albino RPE, the number of melanosomes (closed arrowheads) is reduced and melanosomes are located apically (neural retinal side, Ap RPE) compared with pigmented RPE cells. At the interface of RPE-neural retina, filaments are short and oriented at random in albino retina compared with pigmented retina (open arrowheads). Bs, Basal RPE; Ap, Apical RPE; NR, neural retina. Arrow, dividing retinal cells. Scale bar: 2 μm. **B**: Melanosome density in pigmented (P) and albino (A) RPE at E13.5, E16.5, and E18.5 in

ventrotemporal (VT) and dorsoventroal (DT) regions. At E13.5 VT region, there is a trend of reduction in melanosomes in albino RPE. The reduction trends in albino RPE are observed in the VT and DT region by E18.5. **C**: Melanosome distribution in the apical (neural retinal side) aspects of RPE cells, as a percentage of the total number melanosomes. **B, C**: P, pigmented RPE; A, albino RPE; VT, ventotemporal RPE; DT, dorsotemporal RPE; Black dots, individual measurements; White dots, average values (± SEM). $n = 3$ pigmented and 3 albino littermate embryos from 2 litters. The total number of melanosomes counted to determine melanosome density and distribution: pigmented = 2107, albino = 1344 at E13.5; pigmented = 3113, albino = 2354 at E16.5; pigmented = 5214, albino = 2371 at E18.5.

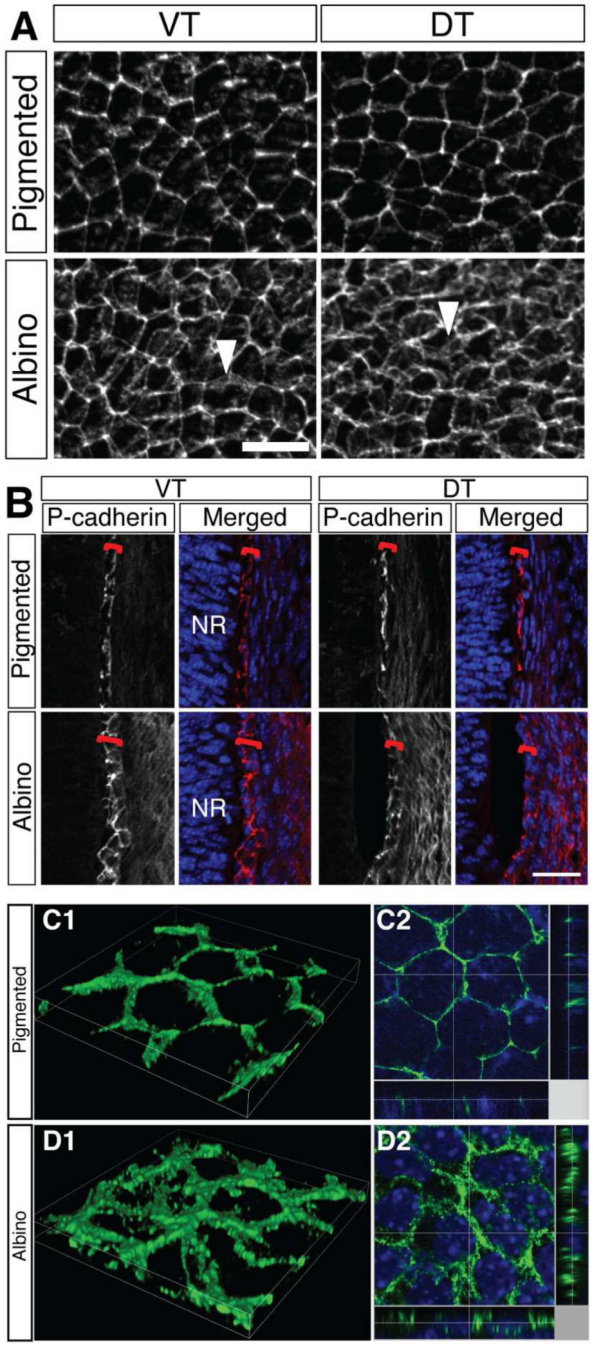

Figure 5. P-cadherin appears diffusely distributed in albino RPE cells

A: RPE flat mount at E15.5 and stained with anti-P-cadherin antibody. In pigmented RPE, P-cadherin outlines RPE cell membrane. In albino RPE, P-cadherin appears more diffuse (arrowheads) in both VT and the DT regions. **B**: Frontal sections of temporal retina at E15.5. P-cadherin labeling outlines RPE (red bracket) in pigmented retina in the VT and the DT regions. In albino RPE, P-cadherin labeling reveals a meshwork rather than an even outline of the cells. NR, neural retina. **C, D**: 3D reconstruction image of VT RPE flat mount at E15.5 stained with anti-P-cadherin antibody. C1, D1, volume image; C2, D2, slice image

(Green, P-cadherin; blue, Hoechst staining). Z-plane images are presented at side. Image area width 34.92 μm, height 34.92 μm. Scale bars: 25 μm (A, B).

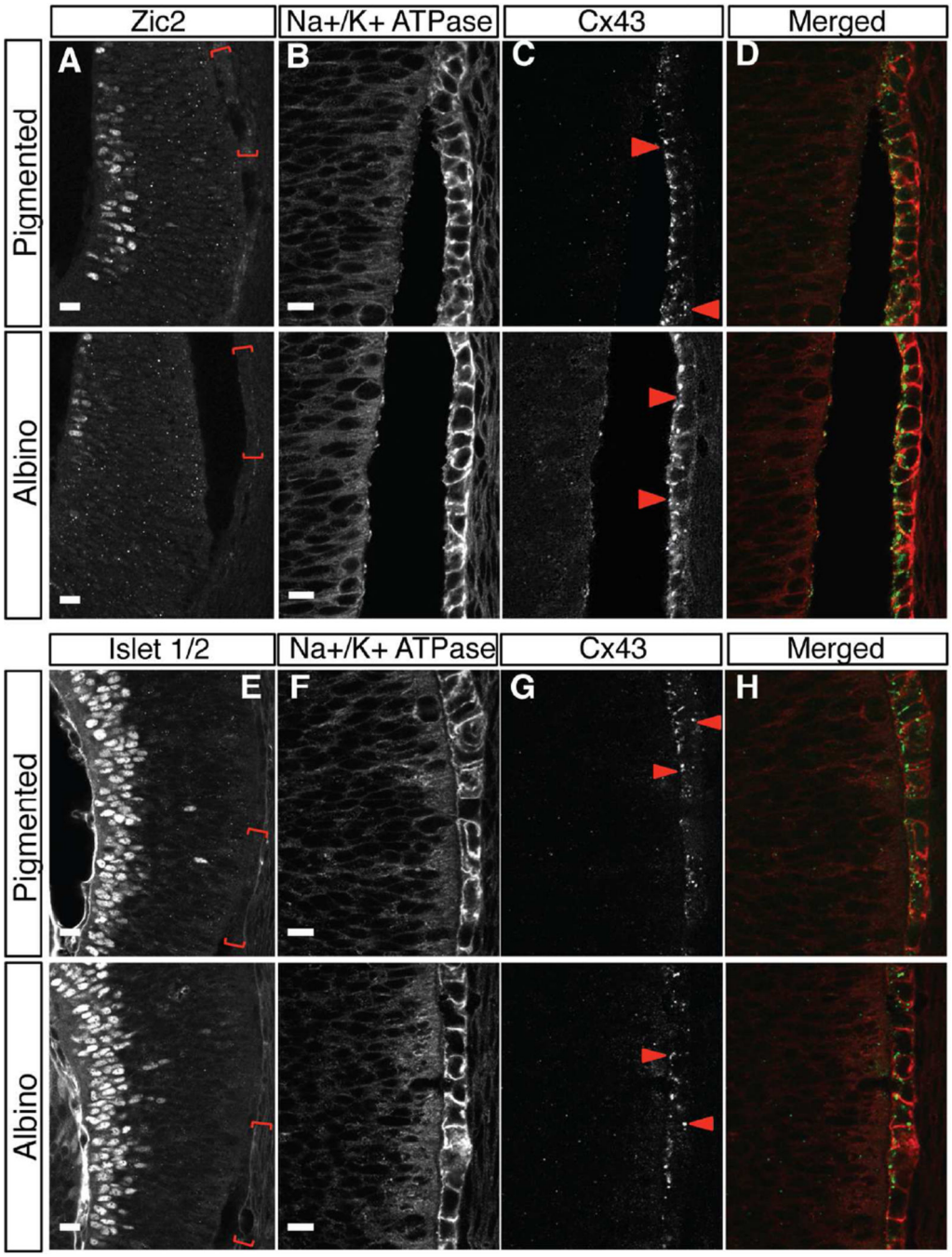

Figure 6. Cx43 is expressed in between RPE cells and at the interface of RPE and neural retina in both albino and pigmented retina

A–H: Frontal retinal sections collected at E15.5 bleached and stained with Zic2 (ipsilateral RGC marker, **A**) or Islet 1/2 (differentiated RGCs, **E**), Na^+/K^+ ATPase (RPE cell membranes, **B, F**) and Cx43 (gap junction, **C, G**). Red bracket regions in Zic2-positive RGC area of the VT region (**A**), or Islet 1/2-positive RGC area of the DT region (**E**) (shown in preceding reference sections) are magnified in panels **B–D** and **F–H**, Cx43 (**C, G**) and merged (**D, H**) micrographs in subsequent panels. Cx43 protein is detected as a punctate

labeling in the RPE and at the interface between RPE and neural retina (arrowheads in **C, G**). Distribution of Cx43 particles is not different between genotypes. Scale bars: 15 μm (**A, E**), 10 μm (**B, C, D, F, G, H**).

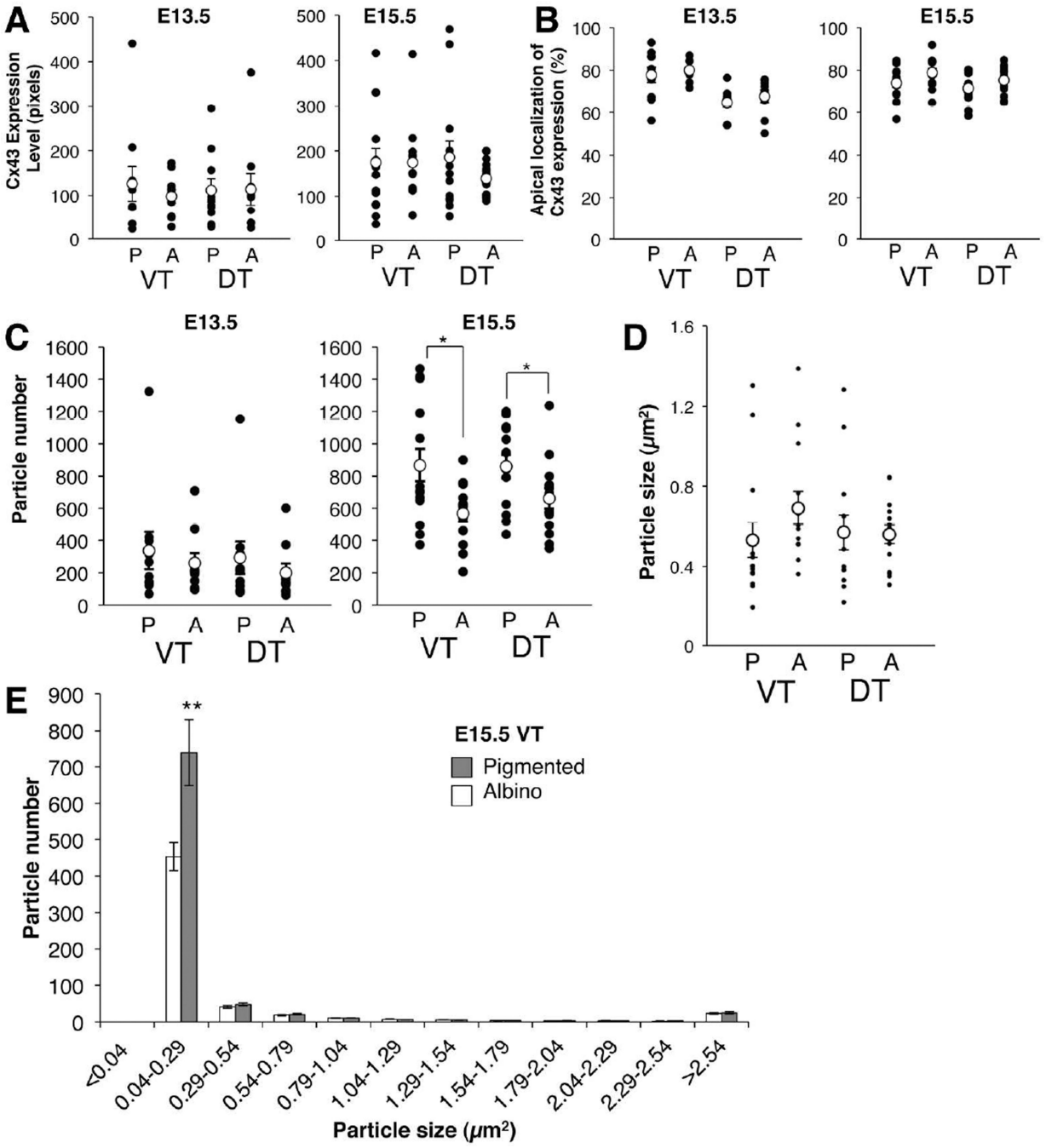

Figure 7. Quantification of Cx43 expression and distribution in RPE cells at E13.5 and E15.5 in VT and DT regions

A: Cx43 expression level, calculated as integrated density of Cx43 labeling/ area of RPE. **B**: Percent of Cx43 expression in the apical or non-apical region of RPE cells. The apical region is defined as the most apical third of the RPE, and the non-apical region is defined as the remaining two-thirds. Percent of Cx43 expression is calculated by dividing Cx43 expression level (analyzed in **A**) within apical region or non-apical region by total Cx43 expression level. **C**: Cx43 particle number in the RPE. **D**: Size of Cx43 particles. **A–D**: P,

pigmented RPE; A, albino RPE; VT, ventrotemporal RPE; DT, dorsotemporal RPE; Black dots, individual measurements; white dots, average values (± SEM). **E**: Histogram of Cx43 particle size. Albino RPE have fewer small Cx43 positive particles compared with pigmented RPE. Bars represent mean (± SEM). *$P < 0.05$, ** $P = 0.01$ (actual P values: **A**. E13.5 VT $P > 0.999$, DT $P > 0.999$ by Mann-Whitney test, E15.5 VT $P = 0.5502$ by Mann-Whitney test, DT $P = 0.2408$ by Welch's t test. **B**. E13.5 VT $P = 0.9705$ by Mann-Whitney test, DT $P = 0.4168$ by unpaired t test, E15.5 VT $P = 0.0806$, DT $P = 0.1582$ by unpaired t test. **C**. E13.5 VT $P = 0.9705$, DT $P = 0.4002$ by Mann-Whitney test, E15.5 VT $P = 0.0159$, DT $P = 0.0475$ by unpaired t test. **D**. VT $P = 0.0427$, DT $P = 0.6500$ by Mann-Whitney test. **E**. $P = 0.01$ by Welch's t test). $n = 5$ pigmented embryos and 5 albino littermate embryos from 3 litters at E13.5; 7 pigmented embryos and 7 albino littermate embryos from 5 litters at E15.5.

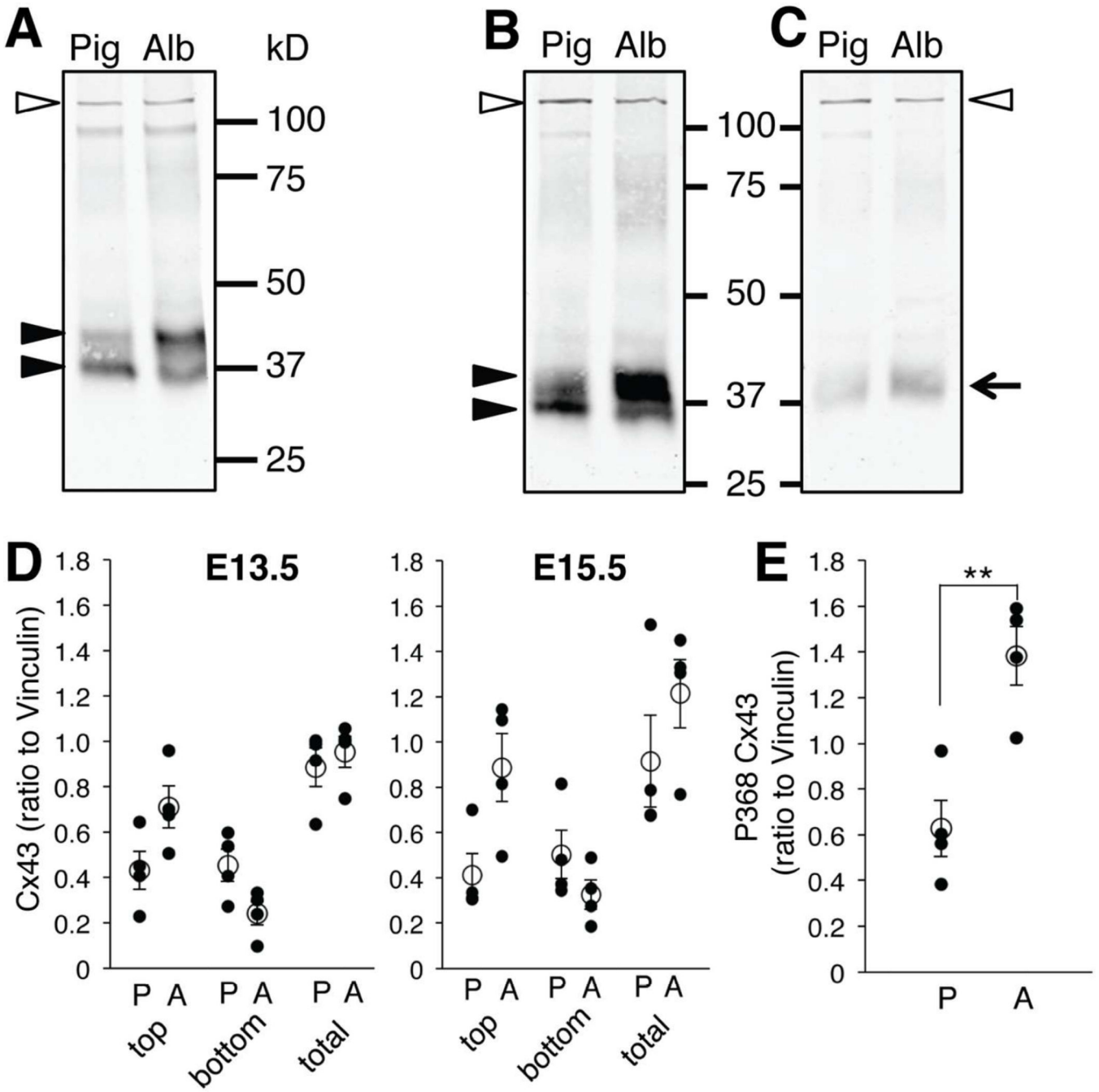

Figure 8. A larger fraction of Cx43 in albino RPE is phosphorylated at serine 368 than in pigmented RPE

A, B: Immunoblot with antibody for total Cx43 consistently distinguished two separate bands (closed arrowheads) in pigmented (Pig) and albino (Alb) RPE extracts at E13.5 (**A**) and E15.5 (**B**). Non-phosphorylated and phosphorylated Cx43 forms correspond to lower and higher bands, respectively (arrowheads). The density of the higher band is greater in albino RPE extracts at E13.5 (**A**) and E15.5 (**B**). **C**: Immunoblot with antibody specific for a phosphorylated Cx43 isoform (P368 Cx43, arrow) showing greater intensity in albino RPE extracts (Alb) compared with pigmented RPE (Pig) at E15.5. Vinculin (117 kD, open

arrowheads) was used to normalize total Cx43 and P368 Cx43 protein in pigmented and albino RPE samples (**A–C**). **D**: Quantification of immnoblot band stained with total Cx43. top, Cx43 higher band; bottom, Cx43 lower band; total, summation of Cx43 higher and lower bands. **E**: Quantification of immnoblot band stained with P368 Cx43. P, pigmented RPE; A, albino RPE. ** $P < 0.01$ by Mann-Whitney test (actual P values: Cx43 E13.5 top $P = 0.0571$, bottom $P = 0.1143$, total $P = 0.3429$. E15.5 top $P = 0.0571$, bottom $P = 0.3429$, total $P = 0.4857$. P368 $P = 0.0286$). $n = 4$ pigmented and 4 albino RPE extract samples.

Table 1

Primary antibodies used in immunohistochemistry (IHC) and western blot (WB).

Antigen	Description of Immunogen	Source, Host Species, Cat. # Clone or Lot#, RRID	Dilution
Zic2	Amino acids 428–530 of human Zic2 (SSGYESSTPPGLVSPSAEPQSSSNLSPAA AAAAAAAAAAAAAVSAVHRGGGSGSG GAGGGSGGGSGSGGGGGGAGGGGGGS SGGGSGTAGGH SGLSSNFNEW)	Brown et al. (2003), rabbit polyclonal, RRID: AB_2315623	1:10,000 (IHC)
Islet1/2	C-terminus portion amino acids 178-349 of rat Islet1 (Karlsson et al.,1990) (PEKTTRVRTVLNEKQLHTLRTCYAANPR PDALMKEQLVEMTGLSPRVIRVWFQNKR CKDKKRSIMMKQLQQQQPNDKTNIQGMT GTPMVAASPERHDGGLQANPVEVQSYQP PWKVLSDFALQSDIDQPAFQQLVNFSEGG PGSNSTGSEVASMSSQLPDTPNSMVASPIE A)	Developmental Studies Hybridoma Bank, mouse monoclonal, contributed by T. Jessell, clone 39.4D5, RRID: AB_528173	1:100 (IHC)
Connexin 43	C-terminus portion amino acids 332-382 of human Connexin 43, Accession# P17302 (AQPFDFPDDNQNSKKLAAGHEL QPLAIVDQRPSSRASSRASSRPRP DDLEI)	Santa Cruz Biotechnology, goat polyclonal, Cat# sc-6560, clone C-20, RRID: AB_638639	1:200 (IHC)
Na+K+-ATPase	Recombinant protein corresponding to amino acids 551–850 of human Na+/K+-ATPase a1	Santa Cruz Biotechnology, rabbit polyclonal, Cat# sc-28800, RRID: AB_2290063	1:50 (IHC)
ZO-1	Synthetic peptide in the middle region (amino acids 1000–1150) of the ZO-1 protein	Thermo Fisher Scientific, rabbit polyclonal, Cat# 40–2200, RRID: AB_10104693	1:200 (IHC)
Otx2	Recombinant protein corresponding to Met1-Leu289 of human Otx2 Accession # P32243	R and D Systems, goat polyclonal, Cat# AF1979, RRID: AB_2157172	1:200 (IHC)
P-cadherin	Mouse endoderm cell line PSA5-E. Recognizes the 118 kDa P-cadherin by immunoblot (Nose and Takeichi, 1986)	Invitrogen, rat monoclonal, Cat# 132000Z, clone PCD-1, RRID: AB_86574	1:500 (IHC)
Mitf	N-terminal Taq-Sac fragment of human Mi protein (corresponding to amino acids 15–290)	Thermo Scientific, mouse monoclonal Cat# MS-771-P0, clone C5, RRID: AB_141540	1:500 (IHC)
Vinculin	Full length human vinculin from human uterus. Accession #P18206 : recognized the 116 kDa vinculin by immunoblot	Sigma-Aldrich, mouse, monoclonal, Cat# V9131, clone hVIN-1, RRID: AB_477629	1:1000 (WB)
Connexin 43	Synthetic peptide corresponding to the C-terminal segment of the cytoplasmic domain (amino acids 363–382 with N-terminally added lysine) of human/rat connexin43 (PSSRASSRASSRPRPDDLEI)	Sigma-Aldrich, rabbit polyclonal, Cat# C6219, RRID: AB_476857	1:6000 (WB)
Phospho-Connexin 43 (Ser368)	Synthetic phosphopeptide corresponding to residues surrounding Ser368 of human connexin 43 (RPSSRAsSRASS)	Cell Signaling Technology, rabbit polyclonal, Cat# 3511S, RRID: AB_2110169	1:100 (WB)